Journal of Advnaces in Applied Computational Mechanics and Engineering

Volume No. 12

Issue No. 1

January - April 2024

ENRICHED PUBLICATIONS PVT. LTD

S-9, IInd FLOOR, MLU POCKET,
MANISH ABHINAV PLAZA-II, ABOVE FEDERAL BANK,
PLOT NO-5, SECTOR-5, DWARKA, NEW DELHI, INDIA-110075,
PHONE: - + (91)-(11)-47026006

Journal of Advnaces in Applied Computational Mechanics and Engineering

Aims and Scope

Journal of Advances in Applied Computational Mechanics & Engineering is a research journal, which publishes top-level work from all areas of theoretical and applied mechanics including theoretical, computational, and experimental aspects, as well as theoretical modeling,methods of analysis and instrumentation. It includes basic disciplineoriented areas such as dynamics, continuum mechanics, solid and fluid mechanics, structures, heat transfer, tribology, geomechanics, and biomechanics, as well as inter-disciplinary subjects such as new numerical and computational techniques, systems control technology, engineering design tools, manufacturing technology, materials and energy technology, and environmental engineering.

Journal of Advance in Applied Computational Mechanics and Engineering

Journal of Advance in Applied Computational Mechanics and Engineering

(Volume No. 12, Issue No. 1, January - April 2024)

Contents

Effect Of Friction Coeficient On En-31with Different Pin Materials Using Pin-On-Disc Apparatus

Ramakant Rana1, R. S. Walia2‡, Manik Singla3

[1] Research Scholar, Department of Mechanical Engineering,
Delhi Technological University, Delhi, India
e-mail: 7ramakant@gmail.com

[2]Associate Professor, Department of Mechanical Engineering,
Delhi Technological University, Delhi, India
e-mail: waliaravinder@yahoo.com,

[3]Student, Department of Mechanical and Automation Engineering,
Maharaja Agrasen Institute of Technology
Delhi, India
e-mail: 26maniksingla@gmail.com

A B S T R A C T

Alloys of Steel have encompassing application in today's technological industries. The range of physical properties that can be imparted to them is remarkable. Tests were conducted using a pin-on-disc test rig as per International StandardsSpecification G99. Experiments have been carried out to study the Friction Coefficienton EN-31 Steel, while the operational parameters were normal load (N) and RotatingVelocity of pin w.r.t. rotating disk at room temperature. Based on the experiments it is found that Friction Coefficientis strongly dependent on applied load, sliding speed and material. Based on the experiments, better tribological results have been achieved in the starved boundary lubrication mode.

Keywords: Friction Coefficient, Sliding Speed, Pin-On-Disc, Taguchi.

1. INTRODUCTION

Studies have revealed that Friction Coefficient depends on normal load, sliding velocity, type of material, temperature, lubrication and vibration [Chowdhury M. A. et al. (2013), Kato K. (2000), Singh M. et al. (2002), Torres Y. et al. (2004), Iwai Y, et al. (2001), Sharma Kumar Vipin et al. (2016)]. The normal load plays an important role for the variation of friction and wear loss.

In many metal pairs, the Friction Coefficientis low at low loads and a transition occurs to a higher value as the normal load is increased. At low loads, the oxide film effectively separates two metal surfaces and there is little or no true metallic contact, hence the friction coefficient is low. At higher load conditions, the film breaks down, resulting in intimate metallic contact, which is responsible for higher friction [Rabinowicz E. (1995)].

Now days, many materials either sliding or rolling are used in different applications. The increase in demand for light weight and energy efficient materials with high strength, stiffness, and wear resistance lead to the experiment of many materials. EN-31 steel is one type of medium strength steel that is suitable where good allround performance is required. EN-31 is widely used for applications which require better properties than mild steel but does not justify the costs of an alloy steel. EN-31 can be flame or induction hardened to produce a good surface hardness with moderate wears resistance.EN-31 is widely used for many general engineering applications. Typical applications include shafts, studs, bolts, connecting rods, screws, piston rod etc., where Friction Coefficient is responsible for many problems. This leads to experiment the effect of Friction Coefficientof EN 31 steel sliding against various materials at various loading conditions.EN-31 Steel is the most common form of steel and its price is relatively low. The properties provided by this material are acceptable for many applications. Mild steel has a relatively low tensile strength, but it is cheap and malleable; surface hardness can be increased through carburizing. It is often used when large quantities of steel are needed.

The consequences of Friction are many, Itusually cost money, in the form of energy loss and material loss:

A. Friction decreases productivity
B. Friction affect quality of Product
C. Friction causes accident

Classifications of friction components:

1. Force transmitting components:

Some components that are expected to operate without interface displacement are called as force transmitting components.

2. Energy absorption-controlling components:

Some components which require large values of a normal force with intermediate coefficient of friction are known as energy absorption - controlling components such as in brakes and clutches.

3.Quality control components:

Some systems that require constant friction and the components which give constant friction are called as quality control components.

4.Low friction component:

The materials that are expected to operate at maximum efficiency at the time of force

force transmitting like gears in a watch are called as low friction component.

2. EXPERIMENTAL SETUP

Set up used in the study of wear test is capable of producing situation accessing Friction Coefficient of the prepared sample. It consists of a pin on disc, loading panel and controller. The entire test was carried out using a "*pin on disc*" machine with normal condition. The condition has 40-50% relative humidity and a temperature of 32-35°C.

In the due course of the experiment. Friction Coefficientwas measured and calculated by using the given formula:

$$\mu = F_w / L \qquad (1)$$

Here, μ: Friction Coefficient, F_w: Friction (Newton), L= Load (N)

Figure 1: Friction Monitor Used for the Friction Tests

3. EXPERIMENTATION

Experiments were performed using a design matrix generated with the help of Taguchi technique. Three different materials were chosen as pin material which were tested at three different levels of speed and loads. EN-31Steel was taken as the plate material. Pin samples and disc has been cleaned properly before and after each test to prevent any form of corrosion on the surface.

The specimen was held steady and stationary within a holder of the apparatus and the required normal load was applied through lever mechanism as can be seen in the figure 1. The sliding distance was kept at 1.0 km for all tests various levels of the load speed and pin material were listed in table 1.

Table 1: Various levels for input factors

Material	Load	Speed
Aluminium	2 kg	1000
Aluminium	5 kg	1300
Aluminium	8 kg	1600
Brass	2 kg	1300
Brass	5 kg	1600
Brass	8 kg	1000
Mild Steel	2 kg	1600
Mild Steel	5 kg	1000
Mild Steel	8 kg	1300

Table 3: Observations for different set of input factors

Material	Load (Kg)	Speed (RPM)	Friction Coefficient (R_1)	Friction Coefficient (R_2)	Mean
Aluminium	2	1000	0.1342	0.1307	0.1324
Aluminium	5	1300	0.1445	0.1424	0.1434
Aluminium	8	1600	0.1293	0.1322	0.1307
Brass	2	1300	0.2572	0.2879	0.2725
Brass	5	1600	0.2286	0.2113	0.2199
Brass	8	1000	0.4013	0.3842	0.3928
Mild Steel	2	1600	0.1962	0.2067	0.2015
Mild Steel	5	1000	0.2981	0.3071	0.3026
Mild Steel	8	1300	0.2683	0.2678	0.2681

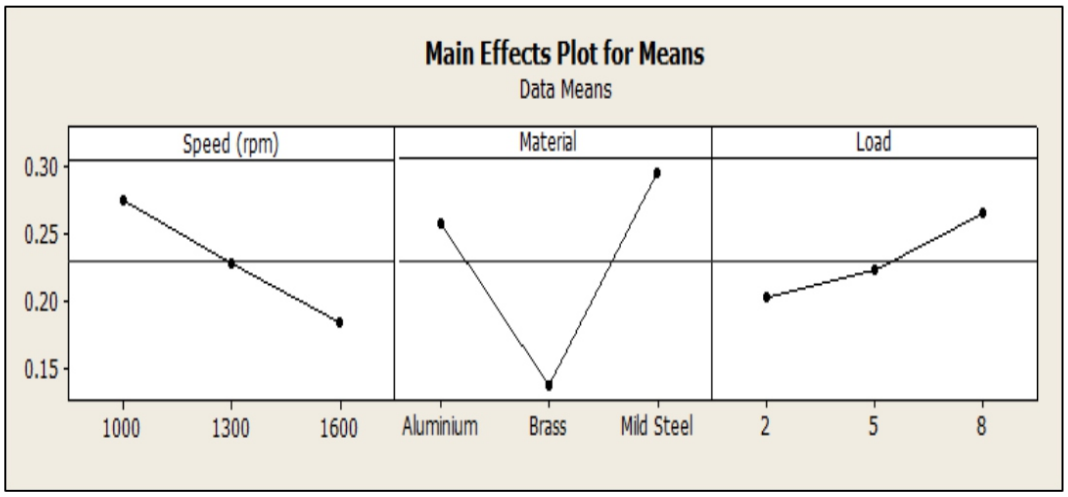

Figure 2: Variation of Wear Rate with Pin Material, Load and Speed.

TABLE 3: Taguchi $L_9(3^4)$ OA (parameters assigned) with response.

Exp. No.	Run order	Parameters Trial Conditions				Responses (Raw Data)		S/N ratio (db)
		A	B	C	-			
		1	2	3	4	**R_1**	**R_2**	
1	3	1	1	1	1	Y_{11}	Y_{12}	S/N (1)
2	7	1	2	2	2	Y_{21}	Y_{22}	S/N (2)
3	5	1	3	3	3	Y_{31}	Y_{32}	S/N (3)
4	1	2	1	3	3	Y_{41}	Y_{42}	S/N (4)
5	4	2	2	1	1	Y_{51}	Y_{52}	S/N (5)
6	6	2	3	2	2	Y_{61}	Y_{62}	S/N (6)
7	9	3	1	2	2	Y_{71}	Y_{72}	S/N (7)
8	2	3	2	1	3	Y_{81}	Y_{82}	S/N (8)
9	8	3	3	3	1	Y_{91}	Y_{92}	S/N (9)
Total						$\sum$	$\sum$	

R_1, R_2, R_3 represent responses values for three repetitions of each trial. The 1's, 2's, and 3's represent levels 1, 2, and 3 of the parameters, which appear at the top of the column. (–) represents no assignment in the column. Y_{ij} are the measured values of the quality characteristic (response).

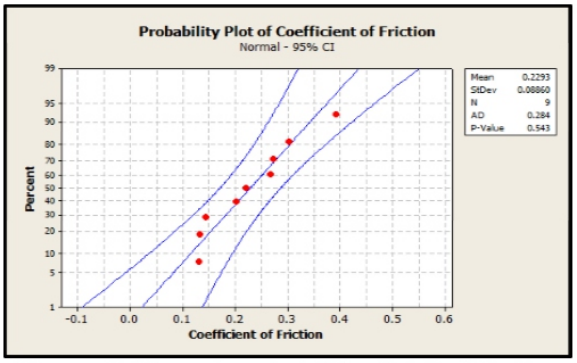

Figure 3: Normal probability plot for Friction Coefficient

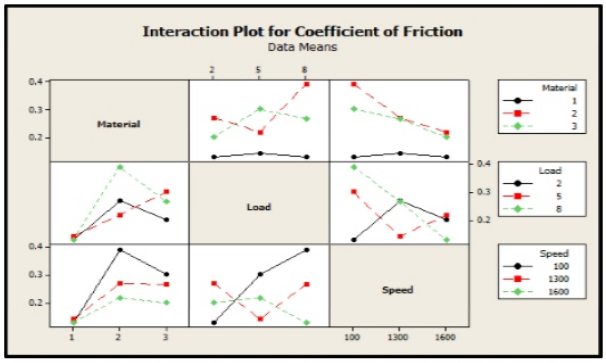

Figure 4: Interaction Plot for Friction Coefficient

4. RESULT AND DISCUSSION

It is clear from the figure 2 that Brass has least Friction Coefficient as compared to Aluminum and Mild Steel as it developed a protective layer in atmospheric conditions [SinglaManoj et al. (2009), Basavarajappa S. et al. (2006)].

The Friction Coefficientincreases with the increase in Load as, at low loads, the oxide film effectively separates two metal surfaces and there is little or no true metallic contact, hence the friction coefficient is low.

At higher load conditions, the film breaks down, resulting in intimate metallic contact, which is responsible for higher friction [Rabinowicz E. (1995)].

The Friction Coefficient decreases with disc speed. Friction increases or decreases as a result of increased sliding velocity for different materials combinations.

An increase in the temperature generally results in metal softening in the case of low melting point metals. An increase in temperature may result in solid-state phase transformation which may either improve or degrade mechanical properties [Sharma Kumar Vipin et al. (2016),Bhushan B. (1999),Dharmalingam S et al. (2011)].

Table 4 shows the responses of Friction Coefficient along with the ranks of the process parameters and Table 2 shows the Taguchi L_9 Orthogonal Array (OA) used in the experimentation [Mandal N. et al. (2012)].

Table 4: Response Table for Friction Coefficient

Level	Material	Load	Speed
1	0.2574	0.2021	0.2759
2	0.1355	0.222	0.228
3	0.2951	0.2639	0.184
Delta	0.1595	0.0617	0.0919
Rank	1	3	2

Figure 3 shows the Normal probability plot for Friction Coefficientand the Figure 4 shows the Interaction Plot for Friction Coefficient. The results in Figure 3 and Figure 4 revealed that the residuals generally fall on a straight line implying that the errors are normal. Figure 3 also revealed that they have a pattern and all the values are in an unusual structure. This implies that the range proposed in the Design of Experiment is adequate and there is no reason to suspect any violation of the independence assumption [Basavarajappa S. et al. (2006)].

Figure 5 shows the Scatter-Plot of Friction Coefficientvs Pin Material, Load and Speed. Figure 5 depicted that Friction Coefficient was least with the Brass in as comparison to the Mild Steel and Aluminium. It also depicted that the Friction Coefficient increases with the increase in Load and decreases with the increase in Speed.

5. CONCLUSION

The material undergoes heavy wear due to sticking of the surfaces as a result of heat generated from friction. The amount of Friction increases as the normal load increases along with the decrease of disc speed. The test pin and the disc exhibits high amount of chatter due to sticking of surfaces.

In this paper, application of Taguchi optimization is applied for the Friction Coefficienton EN-31 Steel is carried out. Taguchi Optimization Technique has been applied for optimizing the Friction Coefficient to investigate the influence of parameters like Load and Speed. The results are as follows:

(1) For the Friction Coefficient, the Pin Materialand the Speed are the main influencing factors on the Friction Coefficient, followed by the Load.

(2) Interaction plots are useful in determining the optimum condition to obtain particular values of Friction Coefficient.

(3) Verification experiments carried out show that the optimized values can be used for obtaining the Friction Coefficientwithin 5% error as can be seen in Normal probability plot for Wear Rate data (Figure 3).

REFERENCES

[1]. K. Kato, Wear in relation to friction - a review, Wear, 241, 2000, 151–157

[2]. M. Singh, D. P. Mondal, O. P. Modi, A. K. Jha, Two body abrasive wear behaviour of aluminum alloy sillimanite particle reinforced composite, Wear, 253, 2002, 357–368

[3]. Y. Torres, S. Rodriguez, A. Mateo, M. Anglada, and L. Llanes, Fatigue behavior of powder metallurgy high speed steels, fatigue limits prediction using a crack growth threshold-based approach, Mater. Sci. Engg. a Structure Mater, 387–389, 2004, 501–4.

[4]. Y. Iwai, T. Honda, H. Yamadaa, T. Matsubara, M. Larsson, S. Hogmarkd, Evaluation of wear resistance of thin hard coatings by a new solid particle impact test, Wear, 251, 2001, 861–867

[5]. Sharma Kumar Vipin, Singh R.C., Chaudhary Rajiv, "wear testing of aluminiumsilicon alloy fabricated by stir casting", isft-2016, id no: 2016-isft- 443, (2016)

[6]. Singlamanoj, Singh Lakhvir, Chawla Vikas, "Study of wear properties of Al-Sic composites", Journal of minerals and materials charactrerisation and engineering, 813-819, (2009)

[7]. Basavarajappa S., Chandramohan G., "Dry sliding wear behaviour of metal matrix composites: a statistical approach", Journal of Materials Engineering and Performance, 656–660, (2006).

[8]. Dharmalingam S, Subramanian R, SomasundaraVinoth K, Anandavel B., "Optimization of tribological properties in aluminium hybrid metal matrix composites using gray-Taguchi method", J Mater Eng Perform,1457–66, (2011)

[9]. Mandal N. , Roy H., B Mondal, Murmu N.C, Mukhopadhyay S.K., "Mathematical modelling of wear characteristics of 6061 Al–alloy–SiC composite using response surface methodology", Journal of Materials Engineering and Performance, 17–24, (2012)

[10]. Chowdhury M. A., Nuruzzaman D. M., Roy B.K., Samad S., Sarker R., "Experimental Investigation of Friction Coefficient and Wear Rate of Composite Materials Sliding against Smooth and Rough Mild Steel Counter faces",Tribology in Industry, Vol.35, No.4, 2013, pp. 286-296.

[11].Rabinowicz E., 1995. Friction and Wear of Materials, 2nd Edition, Wiley.

[12] Bhushan B., 1999. Principle and Applications of Tribology, John Wiley & Sons, Inc.

Effect of Grain Size on Springback in V-bending of Interstitial Free Steel

Vijay Gautam[1], Rohit Shukla[2], Jitendra Singh[3] and D. Ravi Kumar[4]

[1,2,3]Department of Mechanical Engineering,
DTU, Delhi, India
[1] vijay.dce@gmail.com,
[2]the.rohit.shukla@gmail.com
[3] rajwat.jitendrasingh08@gmail.com
[4]Department of Mechanical Engineering,
IIT Delhi, India
[4]dravi@mech.iitd.ac.in

A B S T R A C T

In bending operation, geometrical inaccuracies occur due to springback. To predict the springback, various bending parameters and material properties should be considered. In this paper effect of grain size on springback in V-bending of interstitial free steel has been investigated. To achieve coarse and fine grain sizes, vacuum annealing and oil quenching were adopted respectively. Microstructures of the heat treated specimens were studied to reveal the grain size. The tensile properties of the specimens were tested as per the ASTM-E8M standard. The bend specimens were prepared in the size of 25X150 mm to ensure plane strain bending. The bending experiments were carried out with the help of a punch-die set with a punch profile radius of 12.5mm. Springback results were predicted with FE software and are in close agreement with the experimental results.

Keywords: **Microstructure, Grain size, Annealing, Plane strain bending, Springback.**

1. INTRODUCTION

Bending of sheet metal is a major forming process. In analysis of bending operations, springback is a major concern as it affects the geometrical dimensions of a formed component and leads to lower productivity [1]. Springback is the elastic driven process that adjusts the internal stresses to attain the zero moment and force through sheet thickness [2]. Some major factors such as mechanical properties, tooling geometry & shape and process parameters have been extensively studied to characterize the springback [3-4]. The grain refinement is one of the most effective strengthening mechanisms, improving mechanical properties without loss in ductility [5]. The grain boundary acts as a source of dislocations and the resistance to the dislocation motion from one grain to another. Strength increases with decrease in grain size or vice-versa as discussed by Hall-Petch relationship [6]. In this research, major concern is towards the effect of grain size on mechanical properties which influences the springback. The grain size has been varied successfully by annealing and quenching and its effects on

tensile properties of Interstitial Free (IF) Steel sheet have been studied to design a material model following power law of strain hardening in FE analysis.

2. MICROSTRUCTURE ANALYSIS

The IF Steel strips of dimensions 150mmx25mmx1.2mm were used for the heat treatment to vary the grain size. The two methods used for heat treatment were: Vacuum Annealing and Oil Quenching. Temperature selected for both operations was 850°C. Vacuum annealing was done in a vacuum furnace in a protective atmosphere consisting of 90% of N_2 and 10% of H_2 to prevent oxidation of the samples. Temperature cycle for vacuum annealing is shown in Fig. 1. One set of bend samples were quenched in oil bath to get finer grain size. Microstructure analysis of parent, annealed and quenched specimens was done to reveal the grain sizes & is shown in Fig. 2.

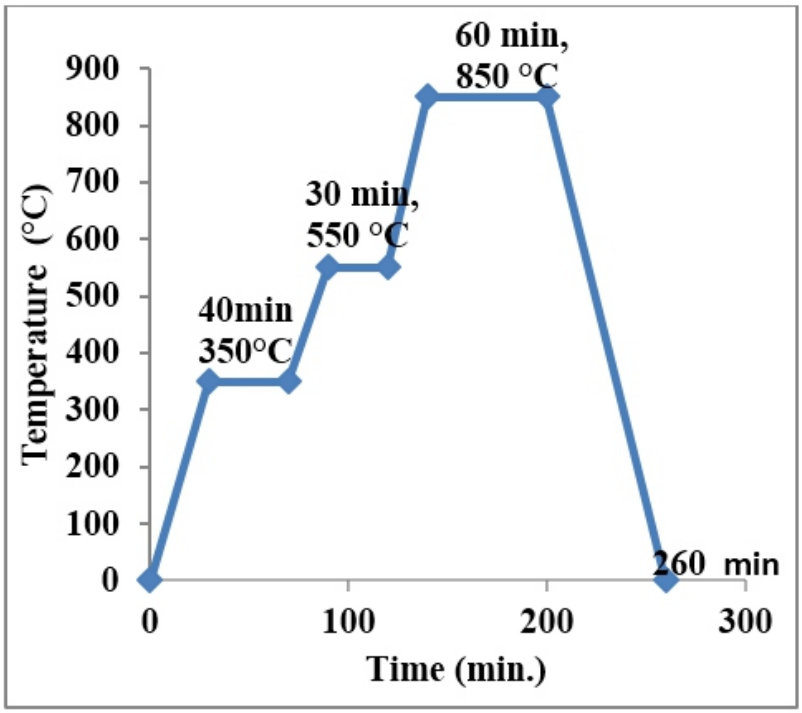

Fig. 1 Temperature cycle for vacuum annealing

The changes in grain size were observed due to heat treatment of sheet metal and were calculated on the basis of linear intercept method. In linear Intercept method, 20 intercepts were considered and then mean of grain size was taken.

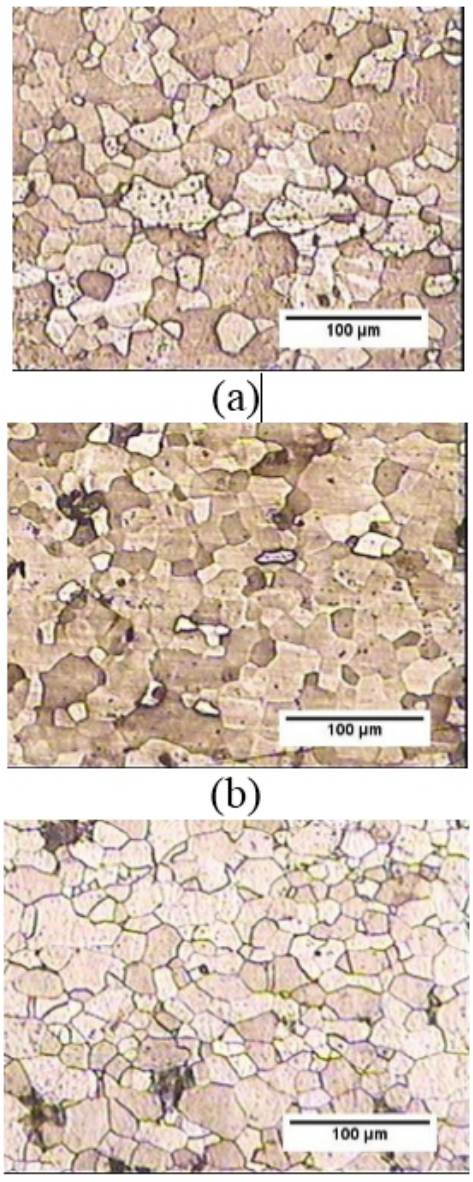

Fig. 2 Microstructure of Interstitial Free Steel: a) Parent, b) Annealed and c) Quenched

3. TENSILE PROPERTIES

The tensile tests were carried out as per ASTM E8M-04 shown in Fig.3 on 50kN table top UTM machine in metal forming laboratory at DTU Delhi. The representative tensile samples of Parent, annealed and quenched IF steel were tested and each test was performed thrice to ensure good reproducibility of the experiments. All the tensile tests were conducted at a cross head speed of 2.54 mm/min. The true stress - true strain curve is plotted for all the specimens and is shown in Fig. 4.

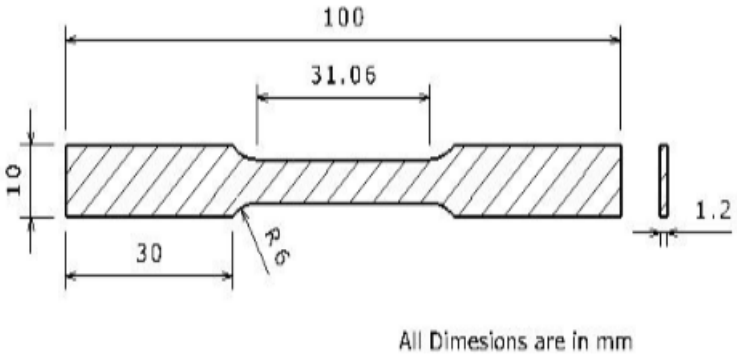

Fig. 3 Tensile Test Specimen according to ASTM E8M-04

The strain hardening exponent (n) and the strength coefficient (K) values were determined from the ln(true stress) Vs ln(true strain) plot in the uniform elongation region.

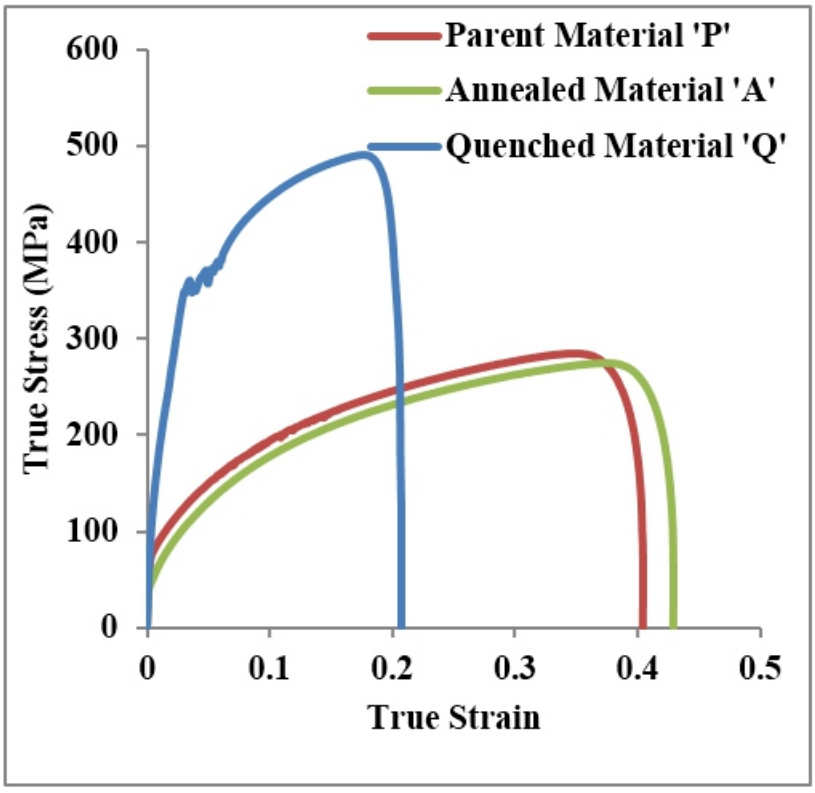

Fig. 4 True Stress Strain curve obtained from tensile test of all Specimens.

4. EXPERIMENTAL SET-UP FOR V-BENDING

The experimental set up as shown in Fig. 5, consists of a punch and die set of D2 steel with included bend angle of 90° and a punch corner radius of 12.5mm. The punch and die set was designed for 50kN UTM. The punch was gripped in the cross head and the die was held by the stationary wedge grip. The bend specimen of size 25X150X1.2mm was freely placed on the die and the punch displacement equal to the die depth was precisely controlled with help of dedicated software.

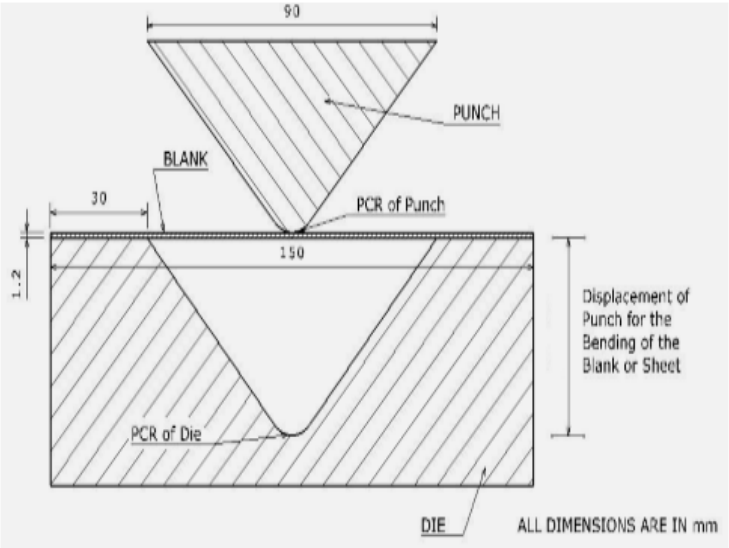

Fig. 5. Complete Set-up of the bending experiment

A clearance of 0.5 mm was provided between the Die and lower surface of blank to prevent any type of localized excess punch force on blank to avoid squeezing action on the sheet thickness.

5. MEASUREMENT OF SPRINGBACK

In bending experiment, the specimens conforms to the shape of the die and therefore included bend angle of the die was used to define the initial bend angle (θ_0) and is equal to 45° for all the experiments. After the removal of deforming load, springback occurs in bent specimens due to elastic recovery of elastic strain and hence angle after springback is defined as final bend angle (θ_f). Initial and final bend angles are determined by Eq. (2) and Eq. (3) respectively. The final included bend angle of the specimens was measured with the help of a coordinate measuring machine (CMM).

Therefore, Spring Back as shown in Fig. 6, can be calculated by subtracting equation (2) from equation (3), we get $\delta = (\theta 0 - \theta f)$

$$\theta_0 = \frac{(180 - \Phi b)}{2} = 45°$$

$$\theta_f = \frac{(180 - \Phi m))}{2}$$

where, Φ_b = Initial Bend Angle (90° for the die) and Φ_m = Measured Bend Angle after springback.

6. FINITE ELEMENT ANALYSIS

Abaqus, an FE software was used for simulations for prediction of springback in V-bending process. The punch and die were modeled as rigid bodies and the blank as deformable with quadrilateral elements. The elastic-plastic Hill's material model obeying power law of strain hardening was adopted for the blank. The Coefficient of friction between Blank and Punch is taken as 0.125 and coefficient of friction between Blank and Die is taken as 0.05. The Modulus of Elasticity is taken as 210 GPa and Poisson's ratio as 0.3. The boundary and loading conditions were imposed on the die and punch. FEA model for springback was solved with Abaqus implicit and is shown in Fig. 6.

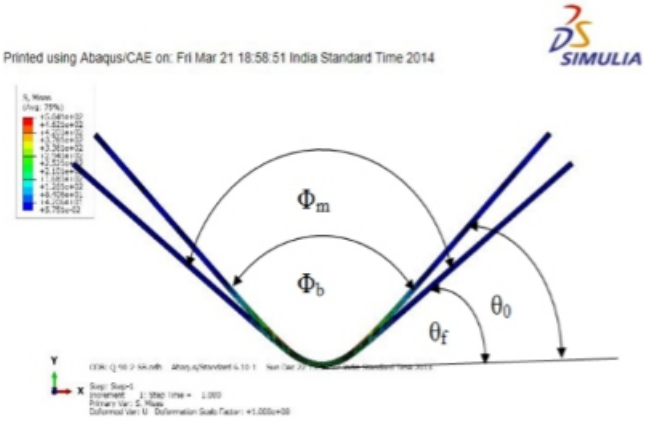

Fig. 6 Overlay plot of simulation of Spring Back

7. RESULTS AND DISCUSSION

Parent material was cold rolled close annealed IF steel with a grain size of 31.33µm. Different heat treatments given to the IF steel successfully varied the grain size and the results for grain size are given in Table 1. Tensile test results shown in Table 2 depicted that coarser grain size results in softer steel with lower tensile strength while the specimens with finer grain size renders the steel comparatively harder and stronger. The percentage elongation is highest for annealed samples and minimum for quenched samples which is a well established fact.

The springback results shown in Table 3 depicts that springback is almost negligible in annealed

specimens but significantly highest in quenched samples.

FE simulation results are in good agreement to the experimental results

Table 1 Grain Size of specimens subjected to heat treatment

Specimen	Parent Specimen	Annealed Specimen	Quenched Specimen
Grain Size (µm)	31.33	35.6	26.2

Table 2 Mechanical Properties of parent material and heat treated samples of IF Steel

Steel samples	Yield Strength (Mpa)	UTS (Mpa)	Strain Hardening Coefficient (n)	Strength Coefficient K(Mpa)	% elongation	Vicker's Hardness No.
Parent	123	205	0.32	428	48.8	91.9HV100
Annealed	117	194	0.33	393	52.9	89.6HV100
Quenched	197	415	0.20	790	21.1	114HV100

0.4°

Table 3 Comparison of Experimental and numerical results of springback

Type of IF Steel	Numerical results	Experimental results
Parent	0.74°	0.4°
Annealed	0.18°	0.04°
Quenched	8.1°	7.97°

8. CONCLUSIONS

Mechanical properties change due to reduction in grain size. It is observed that specimens with coarse grains possess lower hardness, yield strength and higher ductility than that of specimens with finer grains. Annealed samples show a grain size of 35.6µm on an average, whereas quenched samples were observed with grain size of 26.2µm. There is a significant change in the springback value due to the grain size. Coarser grain size in annealed specimens leads to negligible springback suggesting elimination of springback compensation. Whereas, finer grain size depicted very high springback, necessitating significant springback compensation in tooling.

REFERENCES

[1] W. Hosford, R. Caddell, Metal forming: Mechanics and Metallurgy, Prentice Hall, NJ, 1993.

[2] H. Kim, N. Nargundkar, T. Altan, ASME Journal of Manufacturing in Science & Engineering 129 (2007) 342-51.

[3] R. H. Wagoner, M. Li, International journal of Plasticity 23 (2007) 345-60.

[4] M. G. Lee, D. Kin, R. H. Wagoner, K. Chung, ASME Journal of Applied Mechanics 74 (2007) 1264-1275

[5] Krzysztof Muszaka, Jamusz Majta, Lukasz Bienias, Effect of grain refinement of mechanical properties on steels, Journal of Metallurgy and Foundry Engineering – Vol-32 (2006) 87-98.

[6] Hossein Beladi, Gregory S. Rohrer, The Distribution of Grain Boundary of Interstitial Free Steel, The Minerals, Metals and Materials Society and ASM International 2013, Volume 44A.

Effect Of Variation Of High Temperature R1234ze Condenser Temperature And Intermediate R1234yf Temperature Cascade Condenser And Low Temperature Evaporator Circuit In Three Stage Cascade Refrigeration Systems

R S Mishra‡

[1]Department of Mechanical Preoduction & Industrial and Automobiles Engineering,
Delhi Technological University Delhi-110042

e-Mail: hod.mechanical.rsm@dtu.ac.in

[‡] Corresponding Author; Tel: +91-9891079311

A B S T R A C T

The global warming and ozone depletion effects are well documented in the literature causes Climate change through global surface temperatures increase in the last century.For stoping this phenomenon, new regulations in terms of ban of CFC containing chlorine content refrigerants / greenhouse gas fluids (HFC among them) have been approved. Only low-GWP refrigerants will be allowed in developed countries. HFO fluids and most HFCs as refrigerants in HVACR systems possess similar thermo-physical properties such as that the most promising modern refrigerant is R1234ze and R1234yf. In this paper three stage cascade vapour compression refrigeration is proposed for industries (i.e. food, chemical, pharmaceutical and liquefaction of gases) using HFO-1234ze in the high temperature circuit and HFO-1234yf in intermediate temperature circuit and effect of eight ecofriendly refrigerants in the lower temperature circuit and best performance have been using R600 for better system's COP and second law efficiency with minimum exergy destruction ratio. And worst performances (i.e. lowest COP and higher exergy destruction ratio occurs using R407c .The numical computations have been carried out for three stages cascade refrigeration systems and optimum temperature range of components have been observed for optimum performances (i.e.minimum exergy destruction ratio alongwith optimum overall (Maximum System coefficient of performance) occurs) at -45°C of evaporator temperature and -5°C of intermediate cascade evaporator optimum temperature.

Keywords: **Three stage VCR; Reduction in global warming; Ozone depletion; Energy-Exergy computation; first & second law analysis ; Ecofriendly refrigerants**

1. INTRODUCTION

Low temperature cascade refrigeration systems using HFC134a, R507a , HCFC 22 HFC 123 and R508b in the high temperature circuit are normally required in the temperature range from -30°C to -100°C in the various industries such as food, chemical, pharmaceutical and liquefaction of gases such as nitrogen, helium hydrogen etc [1]. The application of multistage vapour compression refrigeration system is also not desirable for attaining very low temperatures due to the solidification temperature of the refrigerant and also low evaporator pressure with larger specific volume along with operational difficulties in the equipment with using single evaporator Gupta et.al [2] optimized the cascaded refrigeration-heat pump system using R-12 refrigerants in the higher temperature circuit and R-13 in low temperature circuit for optimum overall Coefficient of performance. The exergy analysis of multistage cascade refrigeration system for natural gas liquefaction is carried out by Kanoğlu [3] in terms of performance parameters for exergy destruction and exergetic efficiency with minimum work requirement for liquefaction of natural gases.

Dopazo et al. [4] carried out the optimization of coefficient of performance of a cascade refrigeration system for cooling applications at low temperatures. in the variation of evaporation temperature range (- 55°C) to (-30°C) using CO2 in low temperature circuit, 25 to 50°C condensation temperature in high temperature circuit using NH3 and (-)25 to 5°C in cascade condenser. The overlapping (approach temperature) was varied between 3-6°C. The effect of compressor isentropic efficiency on system COP is also examined and also optained optimum condenser temperature. The effect of HFOrefrigerants was not studied by them . Ratts and Brown [5] used the entropy generation minimization method an ideal cascade vapour compression cycle for determining the optimal intermediate temperatures. Bhattacharyya et al. [6] predicted the optimum performance of the cascade system with variation in the design parameters and operating variables by using CO2 in the high temperature cycle of about 120°C and C3H8 (Propane) in the low temperature cycle of about -40°C. Agnew and Ameli [7]used finite time thermodynamics approach for cascade refrigeration system refrigerants R717 in high temperature circuit and R508b low temperature circuit and found better performance in comparison to R12 in high temperature circuit and R13 low temperature. Nicola et al. [8]carried out first law performance analysis using ammonia in high temperature circuit of a cascade refrigeration system , blends of CO2 and HFCs in low temperature circuit of 216.58 K and observed that the ecofriendly CO2 (carbondioxide i.e. R744) blends are excellent options for the low-temperature circuit of cascade systems operating at temperatures arround 200 K. Lee et al. [9]carried out exergy analysis of a two stage cascade refrigeration system for ammonia and carbon dioxide for maximization of COP and minimization of energy loss by optimising condensing temperature and concluded that optimal condensing temperature increased with condensation and evaporation temperatures. Kruse and Rüssmann [10]computed COP of a cascade

refrigeration system using NH3, C3H8, propene, CO2 for the high temperature stage of heat rejection temperatures between 25 to 55 °C and N_2O (Nitrous oxide) as refrigerant in the low temperature cascade stage and compared its result s with a conventional HFC134a cascade refrigeration system and observed that by replacing the lower stage refrigerant R23 by N_2O have same energetic performance with high stage fluids R134a, ammonia and hydrocarbons. Niu and Zhang [11] compared experimental results of a cascade refrigeration system using R290 in high temperature circuit and a blend of R744/R290 in low temperature circuit with performance of with R13 in low temperature circuit and R290 in high temperature circuit and found that good cycle performance of blended R744/R290 in low temperature circuit gives promising performance by replacing R13 refrigerant by blends of R744/R290 when low temperature evaporator temperature is higher than 200 K. Getu and Bansal [10] studied the effect of evaporating, condensing and cascade condenser temperatures, sub-cooling and superheating in high temperature circuits and low temperature circuits and carried out energy analysis of a carbon dioxide– ammonia (R744/R717) cascade refrigeration system using multi-linear regression analysis and developed mathematical expressions for optimum COP using optimum evaporating temperature of R717 and the optimum mass flow ratio of R717 to that of R744 in the cascade system.

2. PERFORMANCE EVALUATION OF THREE STAGES VAPOUR COMPRESSION REFRIGERATION SYSTEM

The three stages cascade vapour compression refrigeration system choosen in this paper has is that tetrafluoropropene (HFO-1234ze) is a hydrofluoroolefin has zero ozone-depletion potential and a low global-warming potential (i.e. GWP = 6) was used in high temperature circuit which has as a "fourth generation" refrigerant to replaceR404a, R407c R-410a in the high temperature circuit in the range of -10°C to 60°C and in the intermediate temperature cycle HFO-1234yf is used because R1234yf is a new class of refrigerant acquiring a global warming potential (GWP) of ($1/335^{th}$) that of R-134a (and around four times higher than carbon dioxide, which can also be used as a refrigerant in the intermediate temperature circuit between (-20°C to -50°C) which has properties significantly different from those of R134a, especially requiring operation at around five times higher pressure) and an atmospheric lifetime of about 400 times shorter. In the low temperature circuit R134a has zero ODP and 1300 GWP is very good Good performance in medium and low temperature applications because of very low toxicity and also not miscible with mineral oil and results were compared by using hydrogen carbon in the low temperature circuit has very promising non-halogenated organic compounds with no ODP and very small GWP values. Their efficiency is slightly better than other leading alternative refrigerants. Iso butane (R 600a) has : ODP-0,GWP-3 has higher boiling point hence lower evaporator pressure and also lowest discharge temperature alongwith very good compatibility with mineral oil. Similarly Propane

(R290 has zero ODP- and -3 GWP is also compatible with copper miscible with mineral oil alongwith highest latent heat and largest vapour densityand third of original charge only is required when replacing halocarbons refrigerant in existing equipmentwith energy saving up to 20% due to lower molecular mass and vapour pressure. The Approximate auto ignition temperatures for R134a is 740 ºC, and For R600a is 470 °C, and For R-290 is 465 °C respectively. The carbon dioxide has Zero ODP & GWP is also non flammable, non toxic, inexpensive and widely available and its high operating pressure provides potential for system size and weight reducing potential has draw back that operating pressure is very high side around 80 bars with low efficiency and only to be used up to -50 °C. The effect of Approach_1 (Overlapping temperature) means intermediate temperature circuit Condenser temperature –high temperature circuit Evaporator temperature and effect of Approach_2 (Overlapping temperature) means Low temperature circuit Condenser temperature –intermediate circuit Evaporator temperature on the performance are also highlighted in this paper.

3. RESULTS AND DISCUSSIONS

Following data have been considered for numerical computation

Condenser Temperature=50 [°C]
Evaporator $_{HTC}$=0.0 [°C]
Evaporator $_{ITC}$=-50.0 [°C]
Evaporator $_{LTC}$=-100.0 [°C]
Compressor Efficiency $_{HTC}$=0.80
Compressor Efficiency $_{ITC}$=0.80
Compressor Efficiency $_{LTC}$=0.80
Approach $_{ITC}$=10[°C]
Approach $_{LTC}$=10[°C]

As overlapping temperature is increasing the total exergy destruction ratio of the system is also increasing. Similarly by increasing low temperature circuit approach the second law efficiency , coefficient of performance of whole system is also decreasing along with decreasing low temperature as coefficient of performance shown in table-1(a) respectively. It was also observed that thre is no effect on COP of high temperature circuit using R1234ze (COP=3.215) and also no effect on COP of intermediate temperature circuit using R1234yf (COP=2.204)and also similarly trends occurred by variation of approach (overlapping temperature between intermediate circuit condenser temperature and high temperature circuit evaporator temperature as shown in Table-1 (b) . As high temperature circuit condenser temperature increases along with total system exergy destruction ratio (EDR) the the overall COP and high temperature circuit COP are also is also decreases along with decreasing exergetic efficiency and no change of coefficient of performances of low temperature circuit (COP=2.204) and coefficient of performance of intermediate temperature circuit COP=1.79 as shown

in Table-2. The table-3 shows the variation of evaporator temperature of high temperature circuit using HFO-1234ze from -20°C to +20°C. It was observed that exergetic efficiency and overall COP of system is increases and exergy destruction ratio decreases first and reached a range to a minimum level and then increases. The optimum performances of cascade systems occurs at intermediate cascade evaporator optimum temperature of -5°C.The variation of cascade evaporator of Intermediate circuit is increasing from -55°C to -30°C, The COP of LTC circuit is decreasing while The COP of ITC circuit is increasing along with increasing exergetic efficiency as shown in Table-4 respectively. It was also observed that there is a optimum (minimum) exergy destruction ratio alongwith optimum overall (Maximum System coefficient of performance) occurs at -45°C.Similarly the increasing temperature of LTC evaporator from -120°C to -90°C , the overall system COP and LTC COPis decreasing and exergy destruction ratio is increasing as shown in Table-5. The effect of various refrigerants used in low temperature circuit is shown in table-6 and it was observed that R600 gives better COP and better second law efficiency with minimum exergy destruction ratio while R407c gives lowest COP and higher exergy destruction ratio. It is seen that use of hydrocarbons are beneficial than using other ecofriendly refrigerants. R-134a is also used up to a temperature -100°C.

Table-1a: Effect of Overlapping temperature of low temperature condenser and Intermediate evaporator temperature Approach in the LTC of three stages Cascade Vapour compression Refrigeration systems using R1234ze in high temperature circuit and R1234yf in Intermediate temperature circuit and R134a in lower temperature circuit for a given data

Approach_ LTC	$COP_{Overall}$	COP_{LTC}	EDR_{System}	ETA_{Second}
0.0	0.570	2.247	1.428	0.4119
2.50	0.5535	2.116	1.50	0.3999
5.0	0.5376	1.998	1.574	0.3884
7.5	0.5222	1.889	1.650	0.3773
10.0	0.5074	1.790	1.728	0.3666

Table-1b: Effect of Approach in the ITC of three stages Cascade Vapour compression Refrigeration systems using R1234ze in high temperature circuit and R1234yf in Intermediate temperature circuit and R134a in lower temperature circuit for a given data

Approach_ ITC	$COP_{Overall}$	COP_{ITC}	EDR_{System}	ETA_{Second}
0.0	0.5675	2.844	1.439	0.410
2.50	0.5522	2.663	1.587	0.3990
5.0	0.5371	2.97	1.577	0.388
7.5	0.5221	2.435	1.651	0.3773
10.0	0.5074	2.204	1.728	0.3666

Table-2: Effect of High temperature circuit condenser temperature in the LTC of three stages Cascade Vapour compression Refrigeration systems using R1234ze in high temperature circuit and R1234yf in Intermediate temperature circuit and R134a in lower temperature circuit for a given data

Condenser Temperature (°C)	Overall System Performance $COP_{Overall}$	High temperature Circuit Performance COP_{HTC}	System Exergy Destruction Ratio EDR_{System}	Exergetic Efficiency ETA_{Second}
60	0.4530	2.47	2.055	0.3273
55	0.4804	2.779	1.881	0.3471
50	0.5074	3.215	1.728	0.3665
45	0.5340	3.737	1.592	0.3859
40	0.5606	4.379	1.469	0.4051
35	0.5873	5.192	1.356	0.4244
30	0.6143	6.264	1.253	0.4438
25	0.6416	7.750	1.157	0.4636

Table-3: Effect the HTC evaporator temperature of three stages Cascade Vapour compression Refrigeration systems using R1234ze in high temperature circuit and R1234yf in Intermediate temperature circuit and R134a in lower temperature circuit for a given data

High Temperature Circuit Evaporator Temperature (°C)	Overall System Performance $COP_{Overall}$	High temperature Circuit Performance COP_{HTC}	System Exergy Destruction Ratio EDR_{System}	Exergetic Efficiency ETA_{Second}
20	0.4698	6.446	1.946	0.3395
15	0.4847	5.287	1.855	0.3502
10	0.4958	4.421	1.791	0.3583
5	0.5033	3.75	1.75	0.3637
0	0.5074	3.275	1.728	0.3666
-5	0.5081	2.78	1.724	0.3671
-10	0.5057	2.42	1.737	0.3654
-15	0.5003	2.117	1.766	0.3615
-20	0.4923	1.86	1.811	0.3557

Table-4: Effect the cascade intermediate evaporator temperature of three stages Cascade Vapour compression Refrigeration systems using R1234ze in high temperature circuit and R1234yf in Intermediate temperature circuit and R134a in lower temperature circuit for a given data

Cascade intermediate Circuit Evaporator Temperature (°C)	Overall System Performance $COP_{Overall}$	High temperature Circuit Performance COP_{ITC}	Low temperature Circuit Performance COP_{LTC}	System Exergy Destruction Ratio EDR_{System}	Exergetic Efficiency ETA_{Second}
-30	0.5023	4.011	1.211	1.755	0.3629
-35	0.5067	3.404	1.328	1.731	0.3661
-40	0.5090	2.921	1.461	1.719	0.3678
-45	0.5092	2.529	1.613	1.718	0.3679
-50	0.5074	2.204	1.798	1.728	0.3666
-55	0.5035	1.931	1.998	1.749	0.3638

Table-5: Effect the Low temperature evaporator temperature(LTC) of three stages Cascade Vapour compression Refrigeration systems using R1234ze in high temperature circuit and R1234yf in Intermediate temperature circuit and R134a in lower temperature circuit for a given data

low Temperature Circuit Evaporator Temperature (^oC)	Overall System Performance $COP_{Overall}$	High temperature Circuit Performance COP_{LTC}	System Exergy Destruction Ratio EDR_{System}	Exergetic Efficiency ETA_{Second}
-90	0.5882	2.40	1.705	0.3697
-95	0.5470	2.067	1.712	0.3687
-100	0.5074	1.79	1.728	0.3666
-105	0.4693	1.556	1.753	0.3632
-110	0.4329	1.358	1.789	0.3586

Table-6: Effect the ecofriendly refrigerants temperature used in low temperature circuit evaporator of three stages Cascade Vapour compression Refrigeration systems using R1234ze in high temperature circuit and R1234yf in Intermediate temperature circuit for a given data

Ecofriendly Refrigerants	Overall System Performance $COP_{Overall}$	High temperature Circuit Performance COP_{HTC}	System Exergy Destruction Ratio EDR_{System}	Exergetic Efficiency ETA_{Second}
R123	0.5099	1.806	1.714	0.3685
R125	0.5020	5.287	1.757	0.3627
R404a	0.4971	4.421	1.784	0.3592
R134a	0.5074	3.75	1.728	0.3666
R407c	0.4367	3.275	2.169	0.3155
R290	0.510	1.807	1.714	0.3685
R600a	0.5123	1.822	1.701	0.3702
R600	0.5148	1.839	1.688	0.3720

4. CONCLUSIONS & RECOMMENDATIONS

The numical computations have been carried out in the three stages cascade refrigeration systems and following conclusions have been made.

1. There is a optimum (minimum) exergy destruction ratio alongwith optimum overall (Maximum System coefficient of performance) occurs at -45°C.
2. The optimum performances of cascade systems occurs at intermediate cascade evaporator optimum temperature of -5°C
3. R600 gives better COP and better second law efficiency with minimum exergy destruction ratio.
4. The minimum performances occurs using R407c gives lowest COP and higher exergy destruction ratio.

REFERENCES

[1] Bansal, P. K. and Jain, Sanjeev(2007), Cascade systems: past, present, and future. ASHRAE Transactions; Vol-113,No.1: pp.245-252.

[2] Gupta V. K. (1985)Numerical optimization of multi-stage cascaded refrigeration-heat pump system. Heat Recovery Systems Vol.5, No.4: pp.305-319.

[3] Kanoğlu M. (2002)Exergy analysis of multistage cascade refrigeration cycle used for natural gas liquefaction. International Journal of Energy Research; Vol.26: pp.763–774.

[4] Dopazo J. A, Fernández-Seara J, Sieres J., Uhía F. J. (2009) Theoretical analysis of a CO2–NH3 cascade refrigeration system for cooling applications at low temperatures. Applied Thermal Engineering ,Vol- 29, No-8-9, pp.1577-1583.

[5] Ratts E.B. and Brown J. S. (2000) A generalized analysis for cascading single fluid vapour compression refrigeration cycles using an entropy generation minimization method. International Journal of Refrigeration Vol.23:,pp.353-365.

[6] Bhattacharyya, S., Mukhopadhyay, S., Kumar A., Khurana R.K. and Sarkar J. (2005) Optimization of a CO2/C3H8 cascade system for refrigeration and heating. International Journal of Refrigeration; Vol.28,pp. 1284- 1292.

[7] Agnew B. and Ameli S.M.(2004)A finite time analysis of a cascade refrigeration system using alternative refrigerants. Applied Thermal Engineering Vol-24: pp.2557–2565.

[8] Nicola G. D., Giuliani, G. , Polonara, F. and Stryjek, R.(2005) Blends of carbon dioxide and HFCs as working fluids for the low-temperature circuit in cascade refrigerating systems. International Journal of Refrigeration; Vol.28: pp.130–140.

[9] Lee T. S., Liu C. H. and Chen T.W.(2006) Thermodynamic analysis of optimal condensing temperature of cascadecondenser in CO2/NH3 cascade refrigeration systems. International Journal of Refrigeration;Vol.29:pp.1100-1108.

[10] Kruse, H. and Rüssmann, H. (2006)The natural fluid nitrous oxide-an option as substitute for low temperature synthetic refrigerants. International Journal of Refrigeration; Vol.29: pp.799-806.

[11] Niu, B. and Zhang, Y.(2007) Experimental study of the refrigeration cycle performance for the R744/R290 mixtures. International Journal of Refrigeration; Vol.30: 37-42.

[12] Getu, H.M., Bansal P.K. (2008); Thermodynamic analysis of an R744/R717 cascade refrigeration system. International Journal of Refrigeration, Vol.31, No.1:,pp.45- 54

Effects of Cetane Improver on Diesel Engine Performance and Emissions

Nitesh Bansal[1‡], Rajiv Choudhary[2] and R. C. Singh[3]

[1]Delhi Technological University, Department of Mechanical Engineering, Student.
bnslboy@gmail.com
[2]Delhi Technological University, Department of Mechanical Engineering, Assistant Professor.
rch_dce@rediffmail.com
[3]Delhi Technological University, Department of Mechanical Engineering, Assistant Professor.
rcsingh@dce.ac.in
[‡] Nitesh Bansal; Tel: +91 8950870033

ABSTRACT

Fossil fuels are diminishing with each and every passing day and there are a lot of emissions from the internal combustion engines. Government in many countries have revised the restricted norms on the usage of the fuel and most of the people also believe in being environment friendly. In India, the cetane number of diesel fuel must be atleast 48 in order to be used in internal combustion engines. Cetane number improvers are added to the fuel in order to enhance its cetane number and help reducing overall Emissions from the engine exhaust. Cetane improver can increase the cetane number upto 12-16 and reduces nitrogen oxides, carbon mono-oxide and unburnt hydrocarbon emissions. Oxygen class cetane improvers such as diethyl ether or 2-ethoxymethyl ether, added in the diesel fuel in about 5~15% concentration can increase the oxygen content of the fuel for better combustion process. And Nitrogen class improvers such as Ethylhexyl Nitrate or cyclohexyl nitrate are used in comparatively smaller quantities ie. 0.1~0.3% in concentration to improve the cetane number of the fuel. In this study review, the effects of cetane improver on the engine performance and emissions are discussed. The study reveals that by using these additives, nitrogen oxides emissions can be reduced upto 20-25%, and hydrocarbon and carbon mono-oxide emissions upto 20 and 25% respectively.

Keywords- Cetane number improver; Diesel Engine; Engine Performance; Engine Emissions; Pollutant; Fuel Additive.

1. INTRODUCTION

Production of fossil fuels is expected to rise, approximately doubling the amount of use of each fossil fuel. As world population continues to grow and the limited amount of fossil fuels begin to diminish, it may not be possible to provide the amount of energy demanded by the world by only using fossil fuels to convert energy. [1]

Burning of fossil fuels causes emissions of nitrogen oxides, carbon mono-oxide, unburnt hydrocarbons and some others. Nitrogen dioxide is an irritant gas, which at high concentrations causes inflammation of the airways. When nitrogen is released during fuel combustion it combines with oxygen atoms to

create nitric oxide (NO). This further combines with oxygen to create nitrogen dioxide (NO_2). Nitric oxide is not considered to be hazardous to health at typical ambient concentrations, but nitrogen dioxide can be. Nitrogen dioxide and nitric oxide are referred to together as oxides of nitrogen (NOx). NOx gases react to form smog and acid rain as well as being central to the formation of fine particles (PM) and ground level ozone, both of which are associated with adverse health effects.[2]

Generally, cetane additive is used in the diesel engine for controlling NOx emissions. There are certain cetane additives used widely such as Ethyl hexyl nitrate, alkyl nitrate, peroxide compounds, methyl oleate.[3]

Cetane number is a measure of the ignition quality of a diesel fuel. It is often mistaken as a measure of fuel quality. Cetane number is actually a measure of a fuel's ignition delay. This is the time period between the start of injection and start of combustion (ignition) of the fuel. In a particular diesel engine, higher cetane fuels will have shorter ignition delay periods than lower cetane fuels. Cetane number should not be considered alone when evaluating diesel fuel quality. API gravity, BTU content, distillation range, sulfur content, stability and flash point are all very important. In colder weather, cloud point and low temperature filter plugging point may be critical factors.[4]

There is no benefit to using a higher cetane number fuel than required. The ASTN Standard Specification for Diesel Fuel Oils (D-975) states, "The cetane number requirements depend on engine design, size, nature of speed and load variations, and on starting and atmospheric conditions. Increase in cetane number over values actually required does not materially improve engine performance. Accordingly, the cetane number specified should be as low as possible to insure maximum fuel availability." This quote underscores the importance of matching engine cetane requirements with fuel cetane number.

Diesel fuels with cetane number lower than minimum engine requirements can cause rough engine operation. They are more difficult to start, especially in cold weather or at high altitudes. They accelerate lube oil sludge formation. Many low cetane fuels increase engine deposits resulting in more smoke, increased exhaust emissions and greater engine wear.

Using fuels which meet engine operating requirements will improve cold starting, reduce smoke during start-up, improve fuel economy, reduce exhaust emissions, improve engine durability and reduce noise and vibration. These engine fuel requirements are published in the operating manual for each specific engine or vehicle.

Overall fuel quality and performance depend on the ratio of parafinic and aromatic hydrocarbons, the presence of sulfur, water, bacteria and other contaminants, and the fuel's resistance to oxidation. The most important measure of fuel quality included API gravity, heat value (BTU content), distillation range and viscosity. Cleanliness and corrosion resistance are also important. For use in cold weather, cloud point and low temperature filter plugging point must receive serious consideration. Cetane number does not measure any of these characteristics.[4]

2. DIESEL EMISSIONS

Diesel engines convert the chemical energy contained in the fuel into mechanical power. Diesel fuel is injected under pressure into the engine cylinder where it mixes with air and where the combustion occurs. The exhaust gases which are discharged from the engine contain several constituents that are harmful to human health and to the environment.

Table 1 lists typical output ranges of the basic toxic material in diesel fumes. The lower values can be found in new, clean diesel engines, while the higher values are characteristic for older equipment.[5]
Table 1. emissions from Diesel engine

CO	HC	DPM	NOx	SO_2
Vppm	vpm	g/m^3	Vppm	vppm
5-1500	20-400	0.1-0.25	50-2500	10-150

Carbon monoxide (CO), hydrocarbons (HC), and aldehydes are generated in the exhaust as the result of incomplete combustion of fuel. A significant portion of exhaust hydrocarbons is also derived from the engine lube oil. When engines operate in enclosed spaces, such as underground mines, buildings under construction, tunnels or warehouses, carbon monoxide can accumulate in the ambient atmosphere and cause headaches, dizziness and lethargy. Under the same conditions, hydrocarbons and aldehydes cause eye irritation and choking sensations. Hydrocarbons and aldehydes are major contributors to the characteristic diesel smell. Hydrocarbons also have a negative environmental effect, being an important component of smog.

Exhaust gases of an engine can have upto 2000 ppm of oxides of nitrogen. Most of this will be nitrogen oxide (NO), with a small amount of nitrogen dioxide (NO_2). NOx is very undesirable. Regulations to reduce NOx emissions continue to become more and more stringent year by year. Released NOx reacts in the atmosphere to form ozone and is one of the major causes of photochemical smog. We would be using different chemicals or additives to improve the cetane number. Therefore, they are termed as

Cetane improvers.

Sulfur dioxide (SO_2) is generated from the sulfur present in diesel fuel. The concentration of SO_2 in the exhaust gas depends on the sulfur content of the fuel. Low sulfur fuels of less than 0.05% sulfur are being introduced for most diesel engine applications throughout the USA and Canada. Sulfur dioxide is a colorless toxic gas with a characteristic, irritating odor. Oxidation of sulfur dioxide produces sulfur trioxide which is the precursor of sulfuric acid which, in turn, is responsible for the sulfate particulate matter emissions. Sulfur oxides have a profound impact on environment being the major cause of acid rains.

Diesel particulate matter (DPM), as defined by the EPA regulations and sampling procedures, is a complex aggregate of solid and liquid material. Its origin is carbonaceous particles generated in the engine cylinder during combustion. The primary carbon particles form larger agglomerates and combine with several other, both organic and inorganic, components of diesel exhaust. Generally, DPM is divided into three basic fractions:

- Solids – dry carbon particles, commonly known as soot,
- SOF – heavy hydrocarbons adsorbed and condensed on the carbon particles, called Soluble Organic Fraction,
- SO_4 – sulfate fraction, hydrated sulfuric acid.

The actual composition of DPM will depend on the particular engine and its load and speed conditions. "Wet" particulates can contain up to 60% of the hydrocarbon fraction (SOF), while "dry" particulates are comprised mostly of dry carbon. The amount of sulfates is directly related to the sulfur contents of the diesel fuel.[5]

3. TYPES OF ADDITIVES

3.1 Oxygen Based Additives

Another group of fuel additives is oxygenated compounds. The idea of using oxygen to produce a cleaner burning of diesel fuels is half a century old. Since that early work, numerous researchers have reported the addition of a variety of oxygenated compounds to diesel fuel. Some oxygenate compounds used are ethanol, acetoacetic esters and dicarboxylic acid esters, ethylene glycol monoacetate, 2-hydroxy Ethyl esters, diethylene glycol dimethyl ether, sorbitan mono-oleate and poly-oxy-ethylene sorbitan mono-oleate, dibutyl maleate and tripropylene glycol monomethyl ether, ethanol and

dimethyl ether, 20 dimethyl ether (DME), dimethyl carbonate (DMC) and dimethoxy methane, 1-octylamino-3-octyloxy-2-propanol and N-octyl nitramine, dimethoxy pro-pane and dimethoxy ethane, and a mixture of methanol and ethanol.[6]

3.2 Nitrogen Based Additives

A common cetane improving additive, 2-ethylhexyl nitrate (2-EHN, EHN), can used to improve diesel fuel ignitability, it is widely used in industries. The chemical formula is $C_8H_{17}NO_3$, with the basic structure an ethyl hexane molecule with one of the hydrogen atoms replaced with an NO3 nitrate radical. EHN is stable at room temperature conditions, and its decomposition reaction rates are even slower when in a fuel solution at high pressure. EHN decomposes at temperatures in the range of 450-550K. Examination of the EHN decomposition process described indicates that NO and NO_2 are formed by the initial decomposition, and the final reaction products include NO. This implies that introducing EHN into the combustion process results in an additional (fuel-borne) NOx formation mechanism that would otherwise not be present.

Substantial prior research concludes that EHN addition does not increase NOx emissions but in many cases actually decreases it. However, these studies were carried out with conventional diesel combustion. Relative to the high levels of NOx produced by conventional diesel combustion, the amount of NOx resulting from EHN decomposition would be insignificant. Increasing fuel cetane number, which occurs when EHN is added, reduces the premixed burn fraction of conventional combustion, leading to lower peak combustion temperatures and decreased thermal NOx formation. This reduction would overshadow any NOx directly formed by EHN decomposition. For combustion processes resulting in low engine-out NOx levels, the amount of NOx formed directly by EHN decomposition may be significant.[7]

4. RESULTS AND DISCUSSIONS

4.1 Effect on BTE and BSFC

Amr Ibrahim analysed the effect on BTE with using diethyl ether as an additive and he found the diesel fuel improved the engine performance significantly as the engine brake thermal efficiency increased and the engine bsfc decreased for the most of engine load conditions. The engine maximum thermal efficiency increased from 32% for the diesel fuel to 32.5%, 34.3%, and 34.3% when the DEE was blended with the diesel fuel with proportions of 5%, 10%, and 15%; respectively. On the other hand, the lowest engine bsfc decreased from 0.252 kg/kW h to 0.247, 0.235, and 0.235 kg/kW h when the DEE was

blended with the diesel fuel with proportions of 5%, 10%, and 15%; respectively.

Alpaslan Atmanly performed an experiment using diesel engine fueled with the blends of diesel, hazelnut oil and he found, higher carbon alcohol and DnBH and DPnH showed slight power loss, attributable to the lower heating values. Decrease in power for DnBH and DPnH was 2.91% and 4.69%, respectively when compared with diesel. The lower heating values of DnBH and DPnH are 41.62 and 41.80 MJ/kg, which are 4.11% and 3.69% lower as compared to diesel. Thus, the average increase of BSFC for DnBH and DPnH was 28.64% and 20.87% as compared to diesel, which is in agreement but it reduced the HC and NOx emissions.

S Imtenan analysed the effect of n-butanol and diethylether on engine performance of a diesel engine fuelled with diesel-jatropha biodiesel blend, J20 and its modified blends with n-butanol showed reasonably higher BSFC than diesel on average. J20 showed on average 5.4% increment of BSFC than diesel. J15B5 and J10B10 showed better BSFC results than J20. They showed on average 2.3% and 3.9% decrement of BSFC than J20. J15D5 and J10D10 showed even better results than n-butanol blends. They showed 5.5% and 6.8% decrement of BSFC than J20 respectively. [8-10]

4.2 Effect on Fuel Properties

In diesel engine fuelled with blends of diesel, hazelnut oil and high carbon alcohol, Alpaslan atmanly concluded the effect of EHN addition, the overall density of diesel fuel was increased. The densities of DnBH and DPnH were 0.8360 and 0.8380 g/ml, which were 1.70% and 1.95% higher, respectively, compared to that of diesel. The addition of EHN to DnBH and DPnH decreased density on a mean of 0.7% and 0.82%, respectively as compared to DnBH and DPnH. Similar changes were observed in kinematic viscosity of the microemulsion fuels.

The addition of EHN to DnBH for the concentrations of 500, 1000 and 2000 ppm shows an increase in cetane number of 4.65%, 13.62% and 21.09%, respectively. Increases of 4.52%, 12.69% and 19.57% were observed for DPnH for the concentrations of 500, 1000 and 2000 ppm, respectively.[9]

4.3 Effect on NOx Emissions

Nicos Ladommatos concluded that as the cetane number increases, the NOx level generally decreases. The decline in the NOx level with increasing cetane number can be explained in terms of decreasing cylinder gas temperature. An increase in the cetane number is accompanied by a reduction in the ignition

delay. In turn, the decreasing ignition delay results in less mixture being involved in premixed combustion, lower peak cylinder gas temperatures and lower NOx formation rates. At low cetane numbers, the injection timing control method has little effect on the NOx level. However, at higher cetane numbers the NOx level becomes dependent on the method of timing control.[11]

Figure 1. shows NOx emissions comparison between pure diesel, B20 (20% biodiesel blend) and B20 with additive.[12]

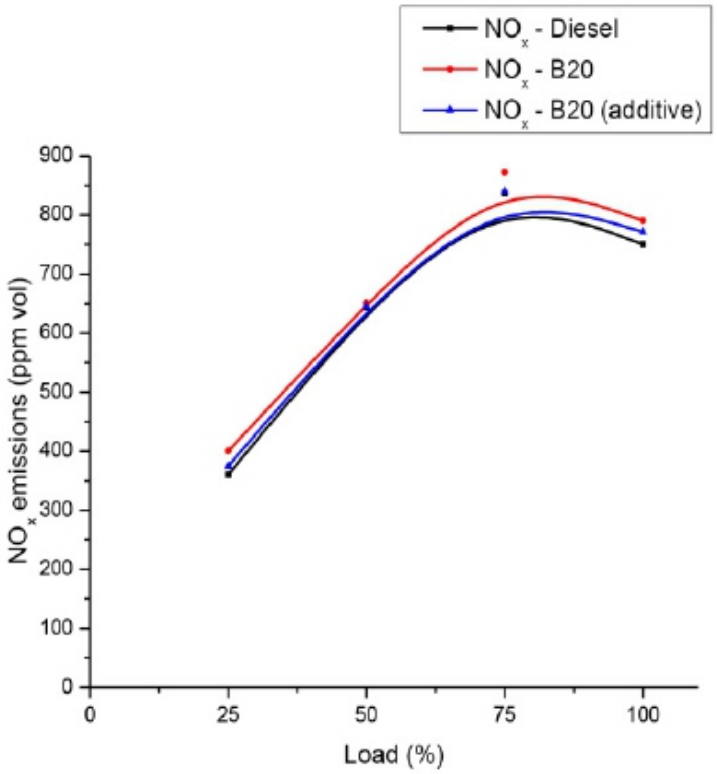

Fig 1. Variation of NOx emissions

The BTHE for B20 was found to be 1.61% higher than fossil diesel when engine was operated at 50% of full load, and 10.79% at higher when operated at full load, the reason being the increase in cetane number by 5.49% in B20 and when compared to fossil diesel.

4.4 Effect on CO Emissions

Carbon monoxide results from the incomplete combustion where the oxidation process does not occur completely. This concentration is largely dependent on air/fuel mixture and it is highest where the excess-air factor (λ) is less than 1.0 that is classified as rich mixture. It can be caused especially at the time of starting and instantaneous acceleration of engine where the rich mixtures are required. In the rich mixtures, due to air deficiency and reactant concentration, all the carbon cannot convert to CO_2 and be formed CO concentration. Although CO is produced during operation in rich mixtures, a small

portion of CO is also emitted under lean conditions because of chemical kinetic effects[13]

It was concluded that in the hazelnut oil and n-butanol/1-pentanol blend CO emissions increased due to lower oxidation of carbon atoms and oxygen molecules as a result of lower in-cylinder temperature, lower oxygen concentration and fuel-rich zones inside the cylinder. DnBH and DPnH blends increased CO emissions with an average of 17.64% and 11.43% as compared to diesel. The main reason for this increase is that n-butanol and 1-pentanol have higher latent heats of evaporation than diesel.

A higher latent of evaporation causes higher evaporative cooling in the combustion chamber, which leads to lower exhaust gas temperature. DnBH and DPnH blends have 19.67% and 17.69% lower cetane numbers than that of diesel. A lower cetane number increases ignition delay and causes accumulation of n-butanol and 1-pentanol in the combustion chamber which require additional heat from the combustion chamber in order to evaporate, creates a cooling effect in the combustion chamber and increases CO emissions.[9]

4.5 Effect on HC Emissions

Hydrocarbon emissions are composed of unburned fuels as a result of insufficient temperature which occurs near the cylinder wall. At this point, the air–fuel mixture temperature is significantly less than the center of the cylinder. Hydrocarbons consist of thousands of species, such as alkanes, alkenes, and aromatics. They are normally stated in terms of equivalent CH_4 content.

Diesel engines normally emit low levels of hydrocarbons. Diesel hydrocarbon emissions occur principally at light loads. The major source of light-load hydrocarbon emissions is lean air–fuel mixing. In lean mixtures, flame speeds may be too low for combustion to be completed during the power stroke, or combustion may not occur, and these conditions cause high hydrocarbon emissions.[13]

In a diesel-Jatropha biodiesel blend, J20 gave significantly lower HC than diesel fuel all over the engine speed range. It gave about 28% decreased emission than diesel on average. Such decrement can be attributed to the higher oxygen content of biodiesel which influenced the amount of hydrocarbon oxidation. On the contrary, J15B5 and J10B10 showed 28.4% and 48% increment of HC emission than J20 on average while J15D5 and J10D10 showed 32% and 52% increment. HC emission was supposed to be reduced due to even higher oxygen content of n-butanol and DEE.[10]

Table 2. Possible Emissions reduction due to the use of Cetane Improvers

Nox	CO	UHC
20-25%	25%	20%

5. ECONOMIC IMPLICATIONS

With the use of cetane improvers, the break thermal efficiency of the engine increases due to better combustion process. Brake Power slightly decreases and so does BSFC but its acceptable because of better exhaust composition of Nitrogen oxides, carbon mono-oxide and unburnt hydrocarbons. Also some widely used cetane improvers like EHN are available easily at cheaper prices and give very good results.

6. CONCLUSION

In this study, this is concluded that a cetane improver really does improve the engine performance and help reducing the emissions. The cetane number of the fuel can be increased 4.52 %, 12.69% and 19.57% by using DPnH in concentrations of 500, 1000 and 2000 ppm respectively. There is a decrease in power for DnBH and DPnH by 2.91% and 4.69%, respectively when compared with diesel but the combustion process gets better. The NOx and HC emissions can be reduced and CO emissions slightly increases but while performing trade off among the emissions, the overall emissions reduces.

Nitrogen Class additives causes wear to the engine but they are more effective as compared to oxygenative additives. Nitrogen class additives such as EHN are used in small concentration ie 0.3~3% and give good results. Oxygen class additives such as DEE are used in comparatively higher concentration ie 5~15% as they do not cause engine wear and give good results. As biodiesel and hazelnut oils blends are used, the cetane number of the fuel decreases and the use of cetane improver becomes necessary.

REFERENCES

[1] Towards Sustainable Energy- http://web.stanford.edu/class/e297c/trade_environment/energy/hfossil.html

[2] Nitrogen Oxide Pollution - Health Effects- http://www.icopal-noxite.co.uk/nox-problem/nox-pollution.aspx

[3] K Velmurugan, S. Gowtham - Effect of Cetane number additives on Emissions-

https://www.google.co.in/url?sa=t&rct=j&q=&esrc=s&source=web&cd=1&cad=rja&uact=8&ved=0ahUKEwj4l9S11__OAhUHLo8KHZfNALUQFgggMAA&url=http%3A%2F%2Fwww.ijmer.com%2Fpapers%2FVol2_Iss

Issue5%2FBL2533723375.pdf&usg=AFAFQjCNGe0-vTEpHPZoLAmFiteaLa0JvWzg&sig2=0GELvJhoLTNqY0HXRf47hw
[4] Fuel-Magic-How does a cetane booster affects the engine performance- http://www.fuelmagic.net/Cetane%20Booster.html
[5] Nettinc - Different types of Diesel emissions- https://www.nettinc.com/information/emissions-faq/what-are-diesel-emissions
[6] Diesel Engine Performance Improvement by Using Cetane Improver- https://www.google.co.in/url?sa=t&rct=j&q=&esrc=s&source=web&cd=1&cad=rja&uact=8&ved=0ahUKEwjn-s-a6v_OAhXMu48KHT7-AAUQFggdMAA&url=http%3A%2F%2Fwww.ijeit.com%2Fvol%25202%2FIssue%252010%2FIJEIT1412201304_36.pdf&usg=AFQjCNFy45npAhn2vYoF2D3OdDdhsrLKgg&sig2=P4pJB-qODsqJqY3R5WhKzQ
[7] Andrew Ickes, Dennis N. Assanis, Stanislav V. Bohac - Effect of 2-Ethylhexyl nitrate on NOx Emissions- https://www.researchgate.net/publication/245235013_Effect_of_2-Ethylhexyl_Nitrate_Cetane_Improver_on_NO_x_Emissions_from_Premixed_Low-Temperature_Diesel_Combustion
[8] Amr Ibrahim - Investigating the effect of using diethyl ether as a fuel additive on diesel engine performance and combustion - http://www.sciencedirect.com/science/article/pii/S1359431116311929
[9] Alpaslan Atmanly - Effects of a cetane improver on fuel properties and engine characteristics of a diesel engine fueled with the blends of diesel, hazelnut oil and higher carbon alcohol- http://www.sciencedirect.com/science/article/pii/S0016236116000223
[10] S Imtenan, HH Masjuki, M. Verman, H. Sajjad - Effect of n-butanol and diethyl ether as oxygenated additives on combustion–emission performance characteristics of a multiple cylinder diesel engine fuelled with diesel–jatropha biodiesel blend- http://www.sciencedirect.com/science/article/pii/S0196890415000515
[11] Nicos Ladommatos, Mohammad Parsi, Angela Knowles - The effect of fuel cetane improver on diesel pollutant emissions - http://www.sciencedirect.com/science/article/pii/0016236194002231
[12] Syed Aatif Avase, Shivank Srivasta - Effect of Pyrogallol as an Antioxidant on the Performance and Emission Characteristics of Biodiesel Derived from Waste Cooking Oil- https://www.researchgate.net/publication/279804774_Effect_of_Pyrogallol_as_an_Antioxidant_on_the_Performance_and_Emission_Characteristics_of_Biodiesel_Derived_from_Waste_Cooking_Oil
[13] Springer - Pollutants Emissions from diesel engine - http://link.springer.com/article/10.1007/s10098-014-0793-9

Energy Analysis and Parametric Study of Flat Pate Collector Area of a Solar Driven Water-Lithium Bromide Half Effect Vapour Absorption Refrigeration System for a given Cooling Load

Abhishek Verma[1], Akhilesh Arora[2], R.S. Mishra[3]

[1]P.G. Student, Mechanical Engineering Department,
Delhi Technological University, Bawana Road Delhi-110042
e-mail- abhishek.ret@gmail.com

[2]Assistant Professor,Mechanical Engineering Department,
Delhi Technological University, Bawana Road
Delhi-110042
e-mail- akhilesharora@dce.ac.in

[3]Professor and Head of Deptt., Mechanical Engineering Department,
Delhi Technological University, Bawana Road Delhi-110042
e-mail- rsmishra1651956@yahoo.co.in

A B S T R A C T

In the modern times,Solar Cooling systems are becoming popular to reduce the carbon footprint of air conditioning. The need and importance of solar based cooling system can play a very prominent role in attenuating energy crisis by the use of solar energy. This paper presents the thermodynamic analysis and calculation of flat plate collector area of vapour absorption half effect cooling system using sun as source of energy. The cooling load is assumed to be 25 kW. The evaporator temperature is maintained constant at 7°C and condenser temperature is varied from 30°C and 46°C and generators temperatures are varied from 65 to 85 °C. For a given condenser temperature (say 38°C) there is an optimum generator temperature for which the total area flat plate collector is minimum. This optimum generator temperature comes out to be 80°C. This generator temperature gives the maximum COP which is obtained as 0.4158. For these values the Area of flat plate collector on High Pressure side (Ah) is 130 m^2.Area of flat plate collector on Low Pressure side (Al) is 154 m^2. Total Area of flat plate collector (A) is 284 m^2.

Keywords- Half Effect, Energy Analysis, Vapour Absorption Refrigeration, Water-Lithium bromide, Flat plate Collector. Solar Driven.

1. INTRODUCTION

At present, the conventional resources of energy are being reduced every day, led to the researchers to identify the systems which use renewable sources of energy. The depletion of conventional sources of energy not only increasing the cost of energy production but also polluting the environment in a severe manner.The refrigeration and air conditioning systems have a major demand of the total energy consumption of the world. The harmful emissions of fossil fuels and chlorine based refrigerants used are responsible for the global warming and the ozone layer depletion. All these problems have led the scientists to develop a refrigeration system which uses renewable sources of energy. The energy of the sun may be harnessed to produce the refrigerating effect which reduces the dependency on high-grade energy and do not pollute the environment.

The primitive characteristic of the half-effect absorption cycle is the running capableness at lower temperatures compared to others. The name "half-effect" rising from the COP, which is almost half that of the single-effect cycle. It must be eminent that COP of the half-effect vapour absorption system is comparatively less as it discard more heat than the absorption cycle working on single-effect, it is approx..50%. However, it can be work with the relatively low temperature heat origin.[1].

Gomri [2] simulated the operation of a half-effect absorption refrigeration system of 10 kW. The energy from the sun is utilized to run the flat plate collector, which are used as the source of heat generation for the vapour absorption refrigeration system. The system has two units, one unit is for the generation of heat which would be utilized to run the second unit i.e. the absorption cooling unit.

Adhikari et al. [3] examined and evaluated the practicability of a vapour absorption refrigeration unit work on solar Energy. The system was designed with the postulate of vapour absorption refrigeration cycle with Lithium Bromide as an absorbing medium and water as a refrigerant.5 kW cooling load for the office building is considered. The designed absorption refrigeration system has COP equitable to 0.77. It proved that the best performance in terms of COP would be succeeded when operated at low generator temperature and the low generator heat. Solar collector area to conduct system is 8 m^2. On the increase of mass flow rate of the refrigerant, the overall cooling effect increases, but the COP decreases. The absorption cooling system is an alternative to the conventional vapour compression system.

Arora et al. [4] carried out the analysis of exergy and energy of half effect lithium bromide water vapor absorption refrigeration system. The optimum intermediate pressure is evaluated to maximize the exergetic efficiency and COP under different conditions. The optimum pressure for both maximum COP and exergy is same. The calculation of optimum pressure involves the effect of high and low pressure temperatures of generator, evaporator, difference of high and low pressure of generator and evaporator, effectiveness of heat exchangers carrying strong and weak solution of Lithium bromide and water. The maximum COP obtained in the range of 0.415 to 0.438,and the value of maximum efficiency is varied from 6.96 to 13.74%.

This paper presents the thermodynamic analysis and calculation of flat plate collector area of vapour absorption half effect cooling system using sun as source of energy.

2. THERMODYNAMIC ANALYSIS OF HALF EFFECT SYSTEM

The half-effect water-lithium (H_2O-$LiBr_2$) bromide vapour absorption refrigeration system, consists

of an condenser, evaporator, LP & HP generators, LP & HP absorbers, LP and HP solution heat exchangers, , solution pumps and solution and refrigerant throttle valves. The condenser and HP generator work at same pressure which is the maximum pressure of the system. The LP generator and HP absorber work at the same intermediate pressure whereas the evaporator and the LP absorber work at same lowermost pressure of the system.

The refrigerant (i.e., water) is circulated through the condenser, evaporator, LP absorber, LP generator, HP absorber, HP generator. When the water vapour has condensed in the condenser, it revert to the evaporator through an expansion valve.

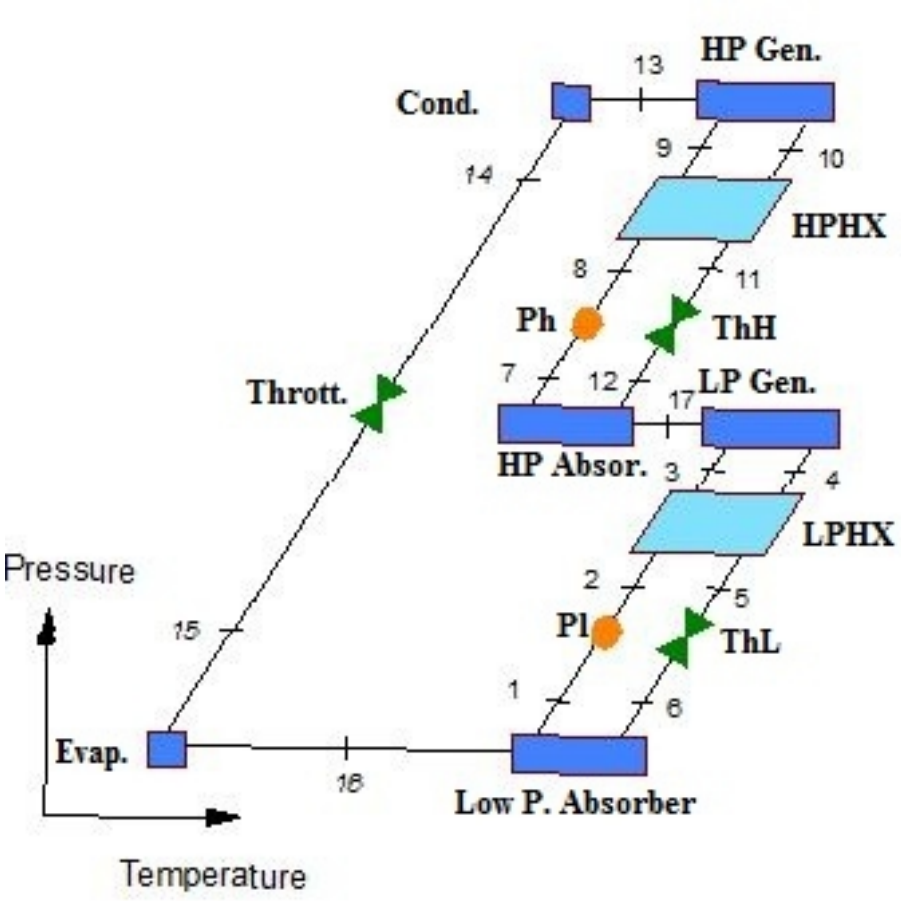

Figure 1 -Block diagram of Half Effect Vapour Absorption Refrigeration System

However, the absorbent that is the lithium bromide aqueous solution is circulated within two distinct stages i.e. the LP stage between the LP generator and the LP absorber, and the HP stage between the HP generator and the HP absorber. Compared to a single-stage vapour absorption refrigeration system, there are two additional components namely LP generator and HP absorber, in a half effect system. These are utilized to concentrate the lithium bromide aqueous solution in the LP stage cycle.

Table 1: p-t-x data for Half effect vapour absorption system

State point	P	T	X	Working fluid state
1.	PE	TAL	X_{Sl}	Equilibrium strong solution LP side
2.	PI	TAL	X_{Sl}	Strong solution
3.	PI	T3	X_{Sl}	Pre heated strong solution
4.	PI	TGL	X_{Wl}	Equilibrium weak solution LP side
5.	PI	T5	X_{Wl}	Sub cooled weak solution
6.	PE	T6	X_{Wl}	Sub cooled weak solution
7.	PI	TAH	X_{Sh}	Equilibrium strong solution HP side
8.	PC	TAH	X_{Sh}	Strong solution
9.	PC	T9	X_{Sh}	Pre heated strong solution
10.	PC	TGH	X_{Wh}	Equilibrium weak solution HP side
11.	PC	T11	X_{Wh}	Sub cooled weak solution
12.	PI	T12	X_{Wh}	Sub cooled weak solution
13.	PC	T13	0	Superheated refrigerant vapour
14.	PC	TC	0	Saturated refrigerant liquid
15.	PE	TE	0	Two phase refrigerant
16.	PE	TE	0	Saturated vapour refrigerant
17.	PI	T17	0	Superheated refrigerant vapour

2.1 Assumptions :

In direction to simulate these absorption refrigeration systems, several assumptions are made, comprehend the succeeding. [5]:

- The analysis of the system is prevailed under steady state conditions.
- The refrigerant (i.e., water) at the exit of the condenser is assumed to be the saturated liquid.
- The refrigerant (i.e., water) at the exit of the evaporator is assumed to be the saturated vapour.
- The Lithium bromide solution at the exit of the absorber is a strong solution and it is at the absorber temperature.
- The exit temperatures from the generator and the absorber from corresponding to equilibrium conditions of the separation and mixing particularly.
- The pressure losses in the pipelines and all the heat exchangers are assumed to be negligible.
- Heat exchange between the surroundings and the system, other than in that is prescribed by heat transfer at the absorber, generator, condenser, evaporator, do not appear.
- The reference state for the system is assumed water at an environment temperature To25°C and 1 atmospheric pressure (Po).
- The system exhibit chilled water.
- The half effect system rejects heat to cooling water at the absorber and the condenser.

2.2 Mass Conservation:

The mass conservation law applied for each component is written as:

$$\sum m_i = \sum m_e \quad (1)$$

This law applied for each component of the cycle is written as:

$$\dot{m}_1 = m_2 = m_3 \quad (2)$$

$$m_4 = m_5 = m_6 \quad (3)$$

$$\dot{m}_7 = m_8 = m_9 \quad (4)$$

$$\dot{m}_{10} = m_{11} = m_{12} \quad (5)$$

$$\dot{m}_{13} = m_{14} = m_{15} = m_{16} = m_{17} \quad (6)$$

LP generator or LP absorber

$$\dot{m}_3 = m_4 + m_{17} \quad (7)$$

HP generator or HP absorber

$$\dot{m}_9 = m_{10} + m_{13} \quad (8)$$

2.3 Conservation of concentration:

The law justifying the concentration conservation for each component is written as:

$$\sum m_i X_i = \sum m_e X_e \qquad (9)$$

Where m is the mass flow rate in the system and X the is mass concentration of lithium bromide in the solution. The law is applied for each component of the cycle is written as:

LP generator or LP absorber

$$m_3X_3 = m_4X_4 \qquad (10)$$

HP generator or HP absorber

$$m_9X_9 = m_{10}X_{10} \qquad (11)$$

$$X_1 = X_2 = X_3, \qquad (12)$$

$$X_4 = X_5 = X_6, \qquad (13)$$

$$X_7 = X_8 = X_9, \qquad (14)$$

$$X_{10} = X_{11} = X_{12}, \qquad (15)$$

$$X_{13} = X_{14} = X_{15} = X_{16} = X_{17} = 0. \qquad (16)$$

3. CALCULATION FOR THE HALF-EFFECT SYSTEM (HVARS):

The computer program is coded in Engineering Equation Solver (EES) for the thermodynamic analysis of HVARS.

In the analysis of this cycle the following assumption is considered

1. The pumping is isentropic
2. Across Solution expansion valve entropy change is neglected and temperature is also constant.

3.1 Input Parameters:

The following are the input parameters to half effect system:

Condenser Temperature TC = 38°C

Evaporator Temperature TE = 7°C

High Pressure side Generator Temperature Tgh = 80°C

Low Pressure side Generator Temperature Tgl = 80°C

High Pressure side Absorber Temperature Tah = 38°C

High Pressure side Absorber Temperature Tah = 38°C

Refrigeration Capacity Qe = 25 kW

Intermediate Pressure Pi = 4.953 kPa

Effectiveness of high pressure side solution heat exchanger EHXh = 0.7

Effectiveness of low pressure side solution heat exchanger EHXl = 0.7

4. CALCULATION OF FLAT PLATE COLLECTOR AREA:

The area of the flat collector is calculated on the basis of the requirement of heat in the two generators. The heat required in the two generators is calculated by the computer based EES program with input parameters given above.

4.1 Flat Plate Collector Specifications:

Dimensions = 2.005mm x 1.505mm

Gross Area (A_F) = 3 m^2

Efficiency (K) = 0.85

Cost = Rs. 6000

The Energy absorbed by the flat plate collector is given as [8] :

$Q = K \times S \times A$ (17)

Where,

K = efficiency of collector plate (K = 0.85)

S = average solar heat falling on earth's surface = 6 kwhr/ m2/day = 250 W/m2

A=Area of Flat Plate collector.

4.2 Calculation Of Area Of Flat Plate Collector For High Pressure Generator :

Heat required in the high pressure generator of the system,
Qgh = 27.48 kW = 27480 W

Hence, the approx. area of the flat plate collector necessary for providing this much amount of energy is given by

$= 27480 / (250 \times K) = 27480 / (250 \times 0.85)$
$= 129.32$ m^2 (i.e.,130 m^2)

Area of Flat Plate collector used in high pressure side (Ah) = 130 m^2

4.3 Calculation Of Area Of Flat Plate Collector For Low Pressure Generator :

Heat required in the low pressure generator of the system,
Qgl = 32.65 kW (i.e, 32650 W)

Hence, the approx. area of the flat plate collector necessary for providing this much amount of energy is given by

$= 32650 / (250 \times K) = 32650 / (250 \times .85)$
$= 153.6\ m^2$(i.e.,154 m^2)

Area of Flat Plate collector used in Low pressure side (Al)= 154 m^2

4.4 Total Area Of Flat Plate Collector (A) :

A = Ah + Al
A = 130 + 145
A = 284 m^2

4.5 Number Of Flat Plate Collectors Required :

Number of Flat Plate Collectors required in High Pressure Side (N1)
$N1 = Ah / A_F = 130/3 = 43.33$
N1 = 44 Plates

Number of Flat Plate Collectors required in Low Pressure Side (N2)
$N2 = Al / A_F = 154/3 = 51.33$
N2 = 52 Plates

5. RESULTS :

The variation of various parameter with respect to generator temperature (TG in °C) at different temperature of condenser (TC) is shown as :

5.1 COP:

The variation of COP with generator temperature is shown in Figure 2. The high values of COP

are hold at high generator temperature and low condenser temperature. For a assumed condenser and evaporator temperature, there is a minimum temperature of generator, which address to the maximum COP. It should be noticed that the COP initially show the significant increase with an increase of generator temperature, and then the slope of the COP curves gets almost flat. In other words, increasing the generator temperature higher than a fixed value does not contribute to much improvement for the COP.

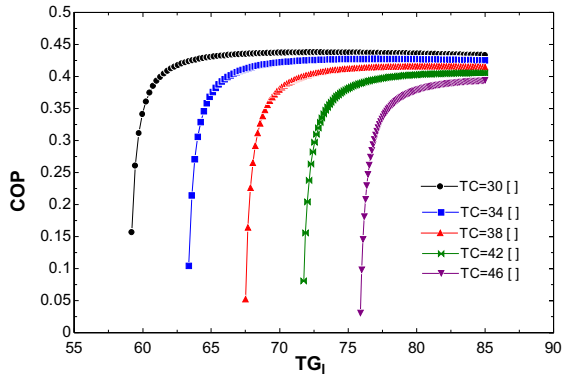

Figure 2 -Coefficient of performance (COP) versus generator temperature (TG in °C) and condenser temperature (TC) at (TE = 7°C)

5.2 Area of flat plate collector on High Pressure side (Ah) :

The variation of Area of flat plate collector on high pressure side is shown in Figure 3. As the generator temperature increases the Ahincreases linearly. When the condenser temperature is increased the value of Ah also increases. In the present study, where the evaporator temperature is maintained fixed at 7°C and condenser temperature is 38°C, generators temperature is 80°C the value of Ah is 130 m^2.

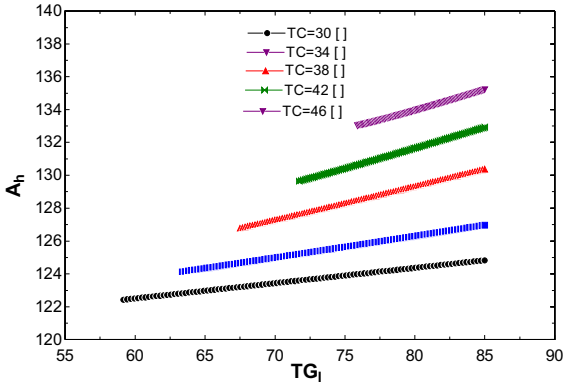

Figure 3 Area of flat plate collector on High Pressure side (Ah in m^2) versus generator temperature (TG in °C) and condenser temperature (TC) at (TE = 7°C)

5.3 Area of flat plate collector on Low Pressure side (Al) :

The variation of Area of flat plate collector on low pressure side is shown in Figure 4. The Al of the absorption cooling system drops keenly to a minimum value with an increase in temperature of generator and then further it approximately remains constant. In the present study, where the evaporator

temperature is maintained fixed at 7°C and condenser temperature is 38°C, generators temperature is 80°C the value of Al is 154 m^2.

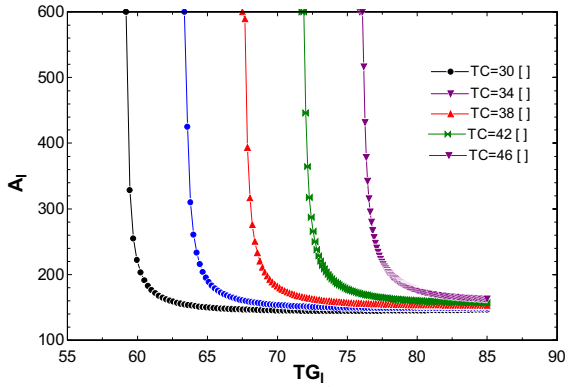

Figure 4 Area of flat plate collector on Low Pressure side (Al in m^2) versus generator temperature (TG in °C) and condenser temperature (TC) at (TE = 7°C)

5.4 Total Area of flat plate collector (A) :

The variation of Total Area of flat plate collector is shown in Figure 5. The A of the absorption cooling system drops keenly to a minimum value with an increase in temperature of generator and then further it approximately remains constant. In the present study, where the evaporator temperature is maintained fixed at 7°C and condenser temperature is 38°C, generators temperature is 80°C the value of A is 284 m^2.

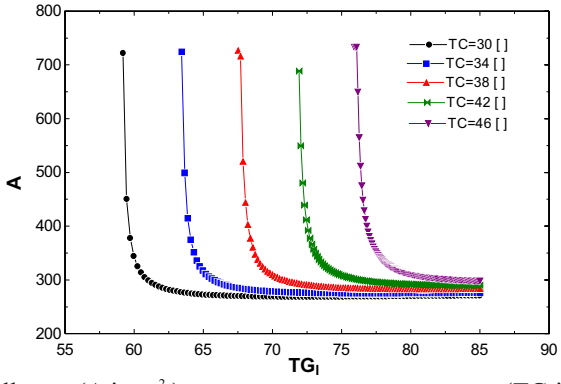

Figure 5 Total Area of flat plate collector (A in m^2) versus generator temperature (TG in °C) and condenser temperature (TC) at (TE = 7°C)

6. CONCLUSIONS:

The main results obtained are concluded below:

- Higher temperature of evaporator and generator, results in higher COP of the system due to the fact that as generator temperature increases, the heat transfer to the solution available in the generator increases, which results in the increase of mass flow rate and so does the COP.

- For the given temperature of condenser there is an optimum temperature of generator for which the total area flat plate collector is minimum. This optimum generator temperature comes out to be 80°C. This generator temperature gives the maximum COP.

- There exists a specific generator temperature below which a half effect system ceases to work. In the present work, this value is found to be 67.51ºC, corresponding to an intermediate pressure of 4.953 kPa (for TC = Tal = Tah = 38°C, TE = 7°C and Tgh = Tgl = 80°C).

- For these values the Area of flat plate collector on High Pressure side (Ah) is 130 m^2.Area of flat plate collector on Low Pressure side (Al) is 154 m^2. Total Area of flat plate collector (A) is 284 m^2.

REFERENCES :

[1] Abdulateef, J.M., 2008, Review on solar-driven ejector refrigeration technologies. Renew SustainEnergy Rev.

[2] RabahGOMRI , (2010). Solar Energy to Drive Half-Effect Absorption Cooling System, Int. J. of Thermal & Environmental Engineering, Volume 1, No. 1 , 1-8.

[3] Jhalak Raj Adhikari, BivekBaral, Ram Lama, BadriAryal, and Roshan Khadka , 2012, Design and analysis of solar absorption air cooling system for an office building Design and analysis of solar absorption air cooling system for an office building, Rentech Symposium Compendium, Volume 2, December.

[4] Akhilesh Arora, Manoj Dixit, and S.C. Kaushik, 2016, Computation Of Optimum Parameters Of A Half Effect Water-Lithium Bromide Vapour Absorption Refrigeration System, Journal of Thermal Engineering, Vol. 2, No. 2, pp. 683-692, April.

[5] Saeed. Sedigh , Hamid. Saffari, 2011, Thermodynamic Analysis Of Single Effect And Half Effect Absorption Refrigeration Systems, International Journal of Energy & Technology Vol. 3 pg 1-9.

[6] Absorption Chillers and Heat Pumps, Second Edition, By Keith E. Herold, ReinhardRadermacher, Sanford A. Klein, 1994.

[7] Jianzhao Wang, Danxing Zheng ,2009, Performance of one and a half-effect absorption cooling cycle of H2O/LiBr system, Energy Conversion and Management Vol. 50, pg 3087–3095.

[8] V.K.Bajpai, 2012, Design of Solar Powered Vapour AbsorptionSystem Proceedings of the World Congress on Engineering 2012 Vol IIIWCE 2012, July 4 – 6, London, U.K.

[9] Refrigeration And Air Conditioning, Third Edition, published by Tata McGraw-Hill Education private Limited, 2012 By C.P. Arora.

[10] Z.F. Li, K. Sumathy, 2000, Technology development in the solarabsorption air-conditioning systems, Renewable and Sustainable Energy Reviews, Vol. 4 pg 267±293.

[11] V Mittal, K S Kasana and N S Thakur, 2006, Modelling and simulation of a solar absorption coolingsystem for India, Journal of Energy in Southern Africa Vol 17 No 3 August.

[12] K. Sumathy , Z. C. Huang And Z. F. Li , 2002, Solar Absorption Cooling With Low Grade Heat Source —A Strategy Of Development In South China, Solar Energy Vol. 72, No. 2, pp. 155–165.

Instructions for Authors

Essentials for Publishing in this Journal

1 Submitted articles should not have been previously published or be currently under consideration for publication elsewhere.

2 Conference papers may only be submitted if the paper has been completely re-written (taken to mean more than 50%) and the author has cleared any necessary permission with the copyright owner if it has been previously copyrighted.

3 All our articles are refereed through a double-blind process.

4 All authors must declare they have read and agreed to the content of the submitted article and must sign a declaration correspond to the originality of the article.

Submission Process

All articles for this journal must be submitted using our online submissions system. http://enrichedpub.com/ . Please use the Submit Your Article link in the Author Service area.

Manuscript Guidelines

The instructions to authors about the article preparation for publication in the Manuscripts are submitted online, through the e-Ur (Electronic editing) system, developed by **Enriched Publications Pvt. Ltd**. The article should contain the abstract with keywords, introduction, body, conclusion, references and the summary in English language (without heading and subheading enumeration). The article length should not exceed 16 pages of A4 paper format.

Title

The title should be informative. It is in both Journal's and author's best interest to use terms suitable. For indexing and word search. If there are no such terms in the title, the author is strongly advised to add a subtitle. The title should be given in English as well. The titles precede the abstract and the summary in an appropriate language.

Letterhead Title

The letterhead title is given at a top of each page for easier identification of article copies in an Electronic form in particular. It contains the author's surname and first name initial .article title, journal title and collation (year, volume, and issue, first and last page). The journal and article titles can be given in a shortened form.

Author's Name

Full name(s) of author(s) should be used. It is advisable to give the middle initial. Names are given in their original form.

Contact Details

The postal address or the e-mail address of the author (usually of the first one if there are more Authors) is given in the footnote at the bottom of the first page.

Type of Articles

Classification of articles is a duty of the editorial staff and is of special importance. Referees and the members of the editorial staff, or section editors, can propose a category, but the editor-in-chief has the sole responsibility for their classification. Journal articles are classified as follows:

Scientific articles:

1. Original scientific paper (giving the previously unpublished results of the author's own research based on management methods).
2. Survey paper (giving an original, detailed and critical view of a research problem or an area to which the author has made a contribution visible through his self-citation);
3. Short or preliminary communication (original management paper of full format but of a smaller extent or of a preliminary character);
4. Scientific critique or forum (discussion on a particular scientific topic, based exclusively on management argumentation) and commentaries. Exceptionally, in particular areas, a scientific paper in the Journal can be in a form of a monograph or a critical edition of scientific data (historical, archival, lexicographic, bibliographic, data survey, etc.) which were unknown or hardly accessible for scientific research.

Professional articles:

1. Professional paper (contribution offering experience useful for improvement of professional practice but not necessarily based on scientific methods);
2. Informative contribution (editorial, commentary, etc.);
3. Review (of a book, software, case study, scientific event, etc.)

Language

The article should be in English. The grammar and style of the article should be of good quality. The systematized text should be without abbreviations (except standard ones). All measurements must be in SI units. The sequence of formulae is denoted in Arabic numerals in parentheses on the right-hand side.

Abstract and Summary

An abstract is a concise informative presentation of the article content for fast and accurate Evaluation of its relevance. It is both in the Editorial Office's and the author's best interest for an abstract to contain terms often used for indexing and article search. The abstract describes the purpose of the study and the methods, outlines the findings and state the conclusions. A 100- to 250-Word abstract should be placed between the title and the keywords with the body text to follow. Besides an abstract are advised to have a summary in English, at the end of the article, after the Reference list. The summary should be structured and long up to 1/10 of the article length (it is more extensive than the abstract).

Keywords

Keywords are terms or phrases showing adequately the article content for indexing and search purposes. They should be allocated heaving in mind widely accepted international sources (index, dictionary or thesaurus), such as the Web of Science keyword list for science in general. The higher their usage frequency is the better. Up to 10 keywords immediately follow the abstract and the summary, in respective languages.

Acknowledgements

The name and the number of the project or programmed within which the article was realized is given in a separate note at the bottom of the first page together with the name of the institution which financially supported the project or programmed.

Tables and Illustrations

All the captions should be in the original language as well as in English, together with the texts in illustrations if possible. Tables are typed in the same style as the text and are denoted by numerals at the top. Photographs and drawings, placed appropriately in the text, should be clear, precise and suitable for reproduction. Drawings should be created in Word or Corel.

Citation in the Text

Citation in the text must be uniform. When citing references in the text, use the reference number set in square brackets from the Reference list at the end of the article.

Footnotes

Footnotes are given at the bottom of the page with the text they refer to. They can contain less relevant details, additional explanations or used sources (e.g. scientific material, manuals). They cannot replace the cited literature.
The article should be accompanied with a cover letter with the information about the author(s): surname, middle initial, first name, and citizen personal number, rank, title, e-mail address, and affiliation address, home address including municipality, phone number in the office and at home (or a mobile phone number). The cover letter should state the type of the article and tell which illustrations are original and which are not.

Address of the Editorial Office:

Enriched Publications Pvt. Ltd.
S-9,IInd FLOOR, MLU POCKET,
MANISH ABHINAV PLAZA-II, ABOVE FEDERAL BANK,
PLOT NO-5, SECTOR -5, DWARKA, NEW DELHI, INDIA-110075,
PHONE: - + (91)-(11)-45525005